

Mice in a labyrinth: Rapid learning, sudden insight, and efficient exploration

Matthew Rosenberg^{1†}, Tony Zhang^{1†}, Pietro Perona², Markus Meister^{1*}

*For correspondence:

mhrosenberg@caltech.edu (MR); tonyzhang@caltech.edu (TZ); perona@caltech.edu (PP); meister@caltech.edu (MM)

¹Division of Biology and Biological Engineering, Caltech, USA; ²Division of Engineering and Applied Science, Caltech, USA

[†]These authors contributed equally to this work

Abstract Animals learn certain complex tasks remarkably fast, sometimes after a single experience. What behavioral algorithms support this efficiency? Many contemporary studies based on two-alternative-forced-choice (2AFC) tasks observe only slow or incomplete learning. As an alternative, we study the unconstrained behavior of mice in a complex labyrinth and measure the dynamics of learning and the behaviors that enable it. A mouse in the labyrinth makes ~2000 navigation decisions per hour. The animal quickly discovers the location of a reward in the maze and executes correct 10-bit choices after only 10 reward experiences – a learning rate 1000-fold higher than in 2AFC experiments. Many mice improve discontinuously from one minute to the next, suggesting moments of sudden insight about the structure of the labyrinth. The underlying search algorithm does not require a global memory of places visited and is largely explained by purely local turning rules.

Introduction

How can animals or machines acquire the ability for complex behaviors from one or a few experiences? Canonical examples include language learning in children, where new words are learned after just a few instances of their use, or learning to balance a bicycle, where humans progress from complete incompetence to near perfection after crashing once or a few times. Clearly such rapid acquisition of new associations or of new motor skills can confer enormous survival advantages.

In laboratory studies, one prominent instance of one-shot learning is the Bruce effect (*Bruce, 1959*). Here the female mouse forms an olfactory memory of her mating partner that allows her to terminate the pregnancy if she encounters another male that threatens infanticide. Another form of rapid learning accessible to laboratory experiments is fear conditioning, where a formerly innocuous stimulus gets associated with a painful experience, leading to subsequent avoidance of the stimulus (*Fanselow and Bolles, 1979; Bourchuladze et al., 1994*). These learning systems appear designed for special purposes, they perform very specific associations, and govern binary behavioral decisions. They are likely implemented by specialized brain circuits, and indeed great progress has been made in localizing these operations to the accessory olfactory bulb (*Brennan and Keverne, 1997*) and the cortical amygdala (*LeDoux, 2000*).

In the attempt to identify more generalizable mechanisms of learning and decision making, one route has been to train laboratory animals on abstract tasks with tightly specified sensory inputs that are linked to motor outputs via arbitrary contingency rules. Canonical examples are a monkey reporting motion in a visual stimulus by saccading its eyes (*Newsome and Pare, 1988*), and a mouse in a box classifying stimuli by moving its forelimbs or the tongue (*Burgess et al., 2017; Guo et al., 2014*). The tasks are of low complexity, typically a 1 bit decision based

on 1 or 2 bits of input. Remarkably they are learned exceedingly slowly: A mouse typically requires many weeks of shaping and thousands of trials to reach asymptotic performance; a monkey may require many months.

What is needed therefore is a rodent behavior that has the hallmark of complex decision making, with many input variables and many possible choices. Ideally the animals would perform this task without excessive intervention by human shaping, so we may be confident that they employ innate brain mechanisms rather than circuits created by the training. Obviously the behavior should be compatible with laboratory experiments. Finally, it would be satisfying if this behavior showed a glimpse of rapid learning.

Navigation through space is a complex behavior displayed by many animals. It typically involves integrating multiple cues to decide among many possible actions. It relies intimately on rapid learning. For example a pigeon or desert ant leaving its shelter acquires the information needed for the homing path in a single episode. Major questions remain about how the brain stores this information and converts it to a policy for decisions during the homing path. One way to formalize the act of decision-making in the laboratory is to introduce structure in the environment in the form of a maze that defines straight paths and decision points. For a burrowing rodent a maze of tunnels is in fact a natural environment. Early studies of rodent behavior did place the animals into true labyrinths (*Small, 1901*), but their use gradually declined in favor of linear tracks or boxes with a single choice point.

We report here on the behavior of laboratory mice in a complex labyrinth of tunnels. The mouse is placed in a home cage from which it has free access to the maze for one night. No handling, shaping, or training by the investigators is involved. By continuous video-recording and automated tracking we observe the animal's entire life experience with the labyrinth. Some of the mice are water-deprived and a single location deep inside the maze offers water. We find that these animals learn to navigate to the water port after just a few reward experiences. In many cases one can identify unique moments of "insight" when the animal's behavior changes discontinuously. This all happens within ~1 hour. Underlying the rapid learning is an efficient mode of exploration driven by some simple navigation rules. Mice that do not lack water show the same patterns of exploration. This laboratory-based navigation behavior may form a suitable substrate for studying the neural mechanisms that implement few-shot learning.

Results

Adaptation to the maze

At the start of the experiment a single mouse was placed in a conventional mouse cage with bedding and food. A short tunnel offered free access to a maze consisting of a warren of corridors (*Figure 1A-B*). The bottom and walls of the maze were constructed of black plastic that is transparent in the infrared. A video camera placed below the maze captured the animal's actions continuously using infrared illumination (*Figure 1B*). The recordings were analyzed offline to track the movements of the mouse, with keypoints on the nose, mid-body, tail base, and the four feet (*Figure 1D*). All observations were made in darkness during the animal's subjective night.

The logical structure of the maze is a binary tree, with 6 levels of branches, leading from the single entrance to 64 endpoints (*Figure 1C*). A total of 63 T-junctions are connected by straight corridors in a design with maximal symmetry (*Figure 1A, Figure 3-figure supplement 1*), such that all the nodes at a given level of the tree have the same local geometry. One of the 64 endpoints of the maze is outfitted with a water port. After activation by a brief nose poke, the port delivers a small drop of water, followed by a 90-s time-out period.

We report observations from 20 animals using a frozen protocol developed from an initial

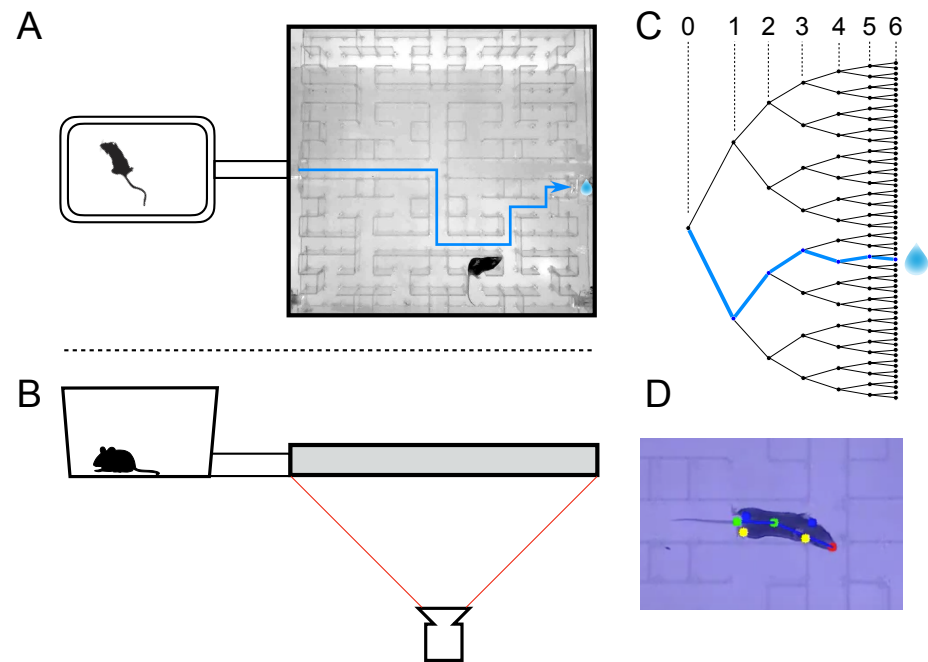


Figure 1. The maze environment. Top (A) and side (B) views of a home cage, connected via an entry tunnel to an enclosed labyrinth. The animal's actions in the maze are recorded via video from below using infrared illumination. (C) The maze is structured as a binary tree with 63 branch points (in levels numbered 0,...,5) and 64 end nodes. One end node has a water port that dispenses a drop when it gets poked. Blue line in A and C: path from maze entry to water port. (D) A mouse considering the options at the maze's central intersection. Colored keypoints are tracked by DeepLabCut: nose, mid body, tail base, 4 feet.

Figure 1–figure supplement 1. Occupancy of the maze.

Figure 1–figure supplement 2. Fraction of time in maze by group.

Figure 1–figure supplement 3. Transitions between cage and maze.

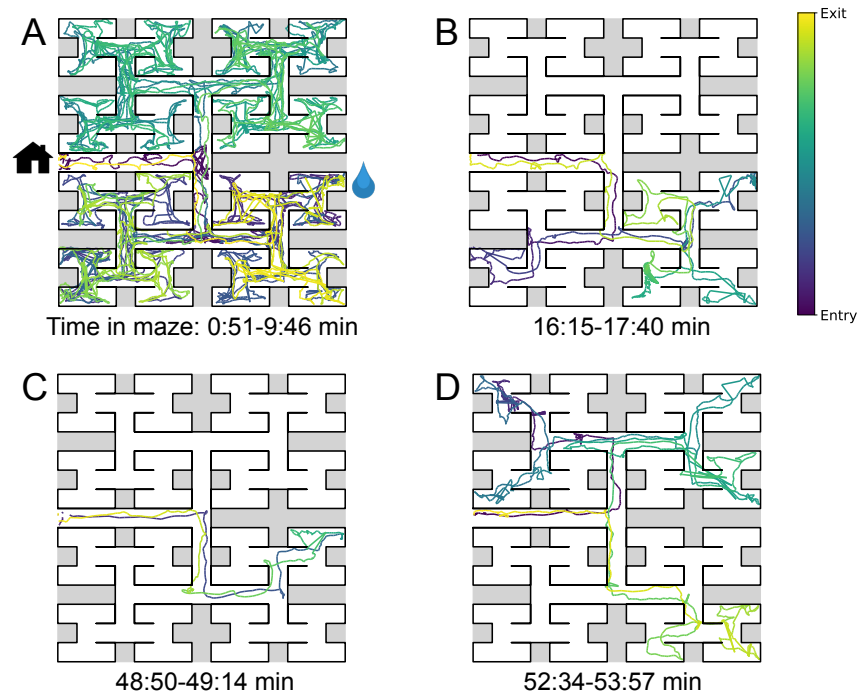


Figure 2. Sample trajectories during adaptation to the maze. Four sample bouts from one mouse (B3) into the maze at various times during the experiment (time markings at bottom). Position of the animal's nose as a function of time during the bout, which is encoded by the color of the trace. In panel A the entrance from the home cage and the water port are indicated with respective symbols.

Figure 2-figure supplement 1. Speed of locomotion.

period of exploratory experiments. Ten of these animals had been mildly water-deprived for 24 hours; they received food in the home cage and water only from the port hidden in the maze. The other ten animals were sated and had free access to food and water in the cage. Each animal's behavior in the maze was recorded continuously for 7 h during the first night of its experience with the maze, starting the moment the connection tunnel was opened (watch a sample video [here](#)). The investigator played no role during this period, and the animal was free to act as it wished including travel between the cage and the maze.

All of the mice except one passed between the cage and the maze readily and frequently (*Figure 1-figure supplement 1*). The single outlier animal barely entered the maze and never progressed past the first junction; we excluded this mouse from subsequent analysis. On average over the entire period of study the animals spent 46% of the time in the maze (*Figure 1-figure supplement 2*). This fraction was similar whether or not the animal was motivated by water rewards (47% for rewarded vs 44% for unrewarded animals). Over time the animals appeared increasingly comfortable in the maze, taking breaks for grooming and the occasional nap. When the investigator lifted the cage lid at the end of the night some animals were seen to escape into the safety of the maze.

We examined the rate of transitions from the cage to the maze and how it depends on time spent in the cage (*Figure 1-figure supplement 3A*). Surprisingly the rate of entry into the maze is highest immediately after the animal returns to the cage. Then it declines gradually by a factor of 4 over the first minute in the cage and remains steady thereafter. This is a large effect, observed for every individual animal in both the rewarded and unrewarded groups. By contrast the opposite transition, namely exit from the maze, occurs at an essentially constant rate throughout the visit (*Figure 1-figure supplement 3B*).

112 The nature of the animal's forays into the maze changed over time. We call each foray
113 from entrance to exit a "bout". After a few hesitant entries into the main corridor, the mouse
114 engaged in one or more long bouts that dove deep into the binary tree to most or all of the
115 leaf nodes (*Figure 2A*). For a water-deprived animal, this typically led to discovery of the
116 reward port. After ~10 bouts, the trajectories became more focused, involving travel to the
117 reward port and some additional exploration (*Figure 2B*). At a later stage still, the animal
118 often executed perfect exploitation bouts that led straight to the reward port and back with no
119 wrong turns (*Figure 2C*). Even at this late stage, however, the animal continued to explore
120 other parts of the maze (*Figure 2D*). Similarly the unrewarded animals explored the maze
121 throughout the night (*Figure 1-figure supplement 2*). While the length and structure of the
122 animal's trajectories changed over time, the speed remained remarkably constant after ~50 s of
123 adaptation (*Figure 2-figure supplement 1*).

124 Whereas *Figure 2* illustrates the trajectory of a mouse's nose in full spatio-temporal detail,
125 a convenient reduced representation is the "node sequence". This simply marks the events
126 when the animal arrives at one of the 127 nodes of the binary tree that describes the maze (see
127 Methods and *Figure 3-figure supplement 1*). Among these nodes, 63 are T-junctions where
128 the animal has 3 choices for the next node, and 64 are end nodes where the animal's only choice
129 is to reverse course. We call the transition from one node to the next a "step". The following
130 investigations all apply to an animal's node sequence.

131 **Few-shot learning of a reward location**

132 We now examine early changes in the animal's behavior that reveal how it rapidly acquires and
133 remembers information needed for navigation. First we focus on navigation to the water port.

134 The ten water-deprived animals had no indication that water would be found in the maze.
135 Yet all 10 discovered the water port in less than 2000 s and requiring fewer than 17 bouts
136 (*Figure 3A*). The port dispensed only a drop of water followed by a 90-s timeout before
137 rearming. During the timeout the animals generally left the port location to explore other parts
138 of the maze or return home. For each of the water-deprived animals, the frequency at which it
139 consumed rewards in the maze increased rapidly as it learned how to find the water port, then
140 settled after a few reward experiences (*Figure 3A*).

141 How many reward experiences are sufficient to teach the animal reliable navigation to the
142 water port? To establish a learning curve one wants to compare performance on the identical
143 task over successive trials. Recall that this experiment has no imposed trial structure. Yet
144 the animals naturally segmented their behavior through discrete visits to the maze. Thus we
145 focused on all the instances when the animal started at the maze entrance and walked to the
146 water port (*Figure 3B*).

147 On the first few occasions these paths to water can involve hundreds of steps between nodes
148 and their length scatters over a wide range. However, after a few rewards, the animals began
149 taking the perfect path without detours (length 6, *Figure 3-figure supplement 1*), and soon
150 that became the norm. Note the path length plotted here is directly related to the number of
151 "turning errors": Every time the mouse turns away from the shortest path to the water port that
152 adds two steps to the path length (*Equation 7*). The rate of these errors declined over time, by
153 a factor of e after ~10 rewards consumed (*Figure 3B*). Late in the night ~75% of the paths to
154 water were perfect. The animals executed them with increasing speed; eventually these fast
155 "water runs" took as little as 2 s (*Figure 3B*). Many of these visits went unrewarded owing to
156 the 90-s timeout period on the water port.

157 In summary, after ~10 reward experiences on average the mice learn to navigate efficiently
158 to the water port, which requires making 6 correct decisions, each among 3 options. Note that
159 even at late times, long after they have perfected the "water run", the animals continue to take

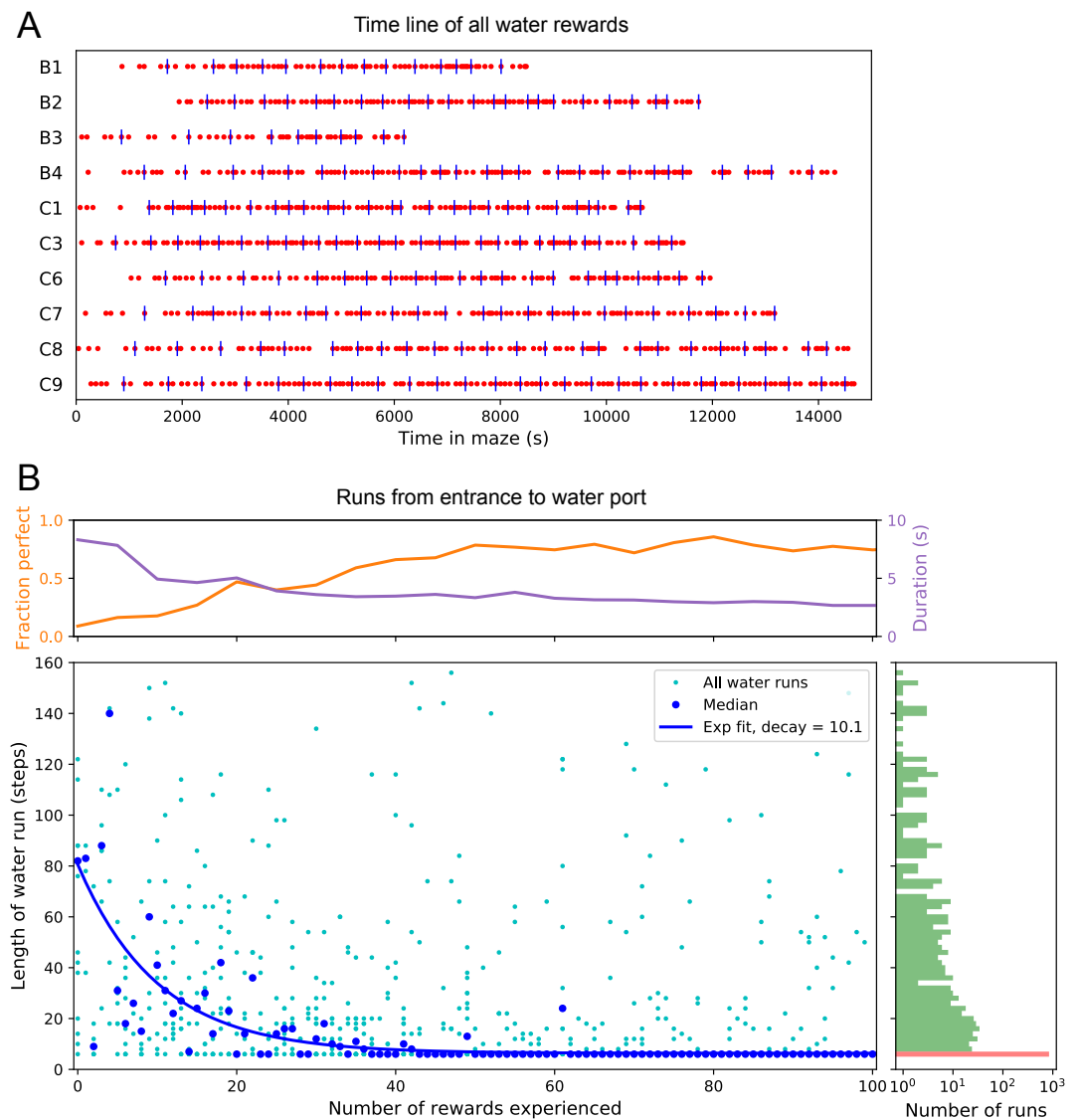


Figure 3. Few-shot learning of path to water. (A) Time line of all water rewards collected by 10 water-deprived mice (red dots, every fifth reward has a blue tick mark). (B) The length of runs from the entrance to the water port, measured in steps between nodes, and plotted against the number of rewards experienced. Main panel: All individual runs (cyan dots) and median over 10 mice (blue circles). Exponential fit decays by $1/e$ over 10.1 rewards. Right panel: Histogram of the run length, note log axis. Red: perfect runs with the minimum length 6; green: longer runs. Top panel: The fraction of perfect runs (length 6) plotted against the number of rewards experienced, along with the median duration of those perfect runs.

Figure 3—figure supplement 1. Definition of node trajectories.

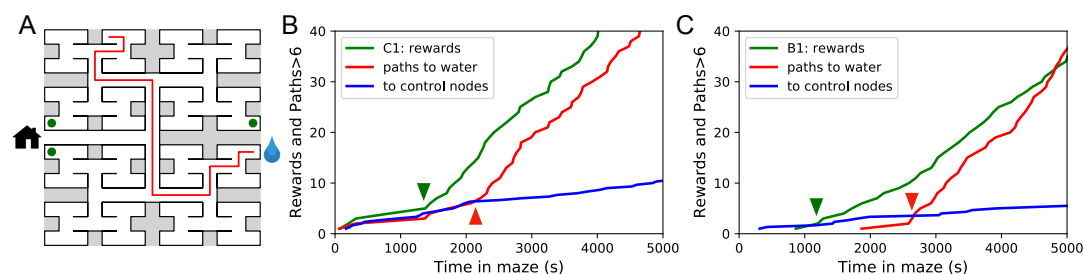


Figure 4. Sudden changes in behavior. (A) An example of a long uninterrupted path through 11 junctions to the water port (drop icon). Circles mark control nodes related by symmetry to the water port to assess the frequency of long paths occurring by chance. (B) For one animal (named C1) the cumulative number of rewards (green); of long paths (>6 junctions) to the water port (red); and of similar paths to the 3 control nodes (blue, divided by 3). All are plotted against the time spent in the maze. Arrowheads indicate the time of sudden changes, obtained from fitting a step function to the rates. (C) Same as B for animal B1.

Figure 4–figure supplement 1. Long direct paths for all animals.

Figure 4–figure supplement 2. Statistics of sudden changes in behavior.

some extremely long paths: a subject for a later section (*Figure 6*).

Discontinuous learning

While an average across animals shows evidence of rapid learning (*Figure 3*) one wonders whether the knowledge is acquired gradually or through moments of “sudden insight”. To explore this we scrutinized more closely the time line of individual water-deprived animals in their experience with the maze. The discovery of the water port and the subsequent collection of water drops at a regular rate is one clear change in behavior that relies on new knowledge. This rate of water rewards can increase rather suddenly (*Figure 3A*), suggesting an instantaneous step in knowledge.

Over time, the animals learned the path to water not only from the entrance of the maze but from many locations scattered throughout the maze. The largest distance between the water port and an end node in the opposite half of the maze involves 12 steps through 11 intersections (*Figure 4A*). Thus we included as another behavioral variable the occurrence of long direct paths to the water port which reflects how directly the animals navigate within the maze.

Figure 4B shows for one animal the cumulative occurrence of water rewards and that of long direct paths to water. The animal discovers the water port early on at 75 s, but at 1380 s the rate of water rewards jumps suddenly by a factor of 5. The long paths to water follow a rather different time line. At first they occur randomly, at the same rate as the paths to the unrewarded control nodes. At 2070 s the long paths suddenly increase in frequency by a factor of 5. Given the sudden change in rates of both kinds of events there is little ambiguity about when the two steps happen and they are well separated in time (*Figure 4B*).

The animal behaves as though it gains a new insight at the time of the second step that allows it to travel to the water port directly from elsewhere in the maze. Note that the two behavioral variables are independent: The long paths don’t change when the reward rate steps up, and the reward rate doesn’t change when the rate of long paths steps up. Another animal (*Figure 4C*) similarly showed an early step in the reward rate (at 860 s) and a dramatic step in the rate of long paths (at 2580 s). In this case the emergence of long paths coincided with a modest increase (factor of 2) in the reward rate.

Similar discontinuities in behavior were seen in at least 5 of the 10 water-deprived animals (*Figure 4–figure supplement 1*, *Figure 4–figure supplement 2*), and their timing could be

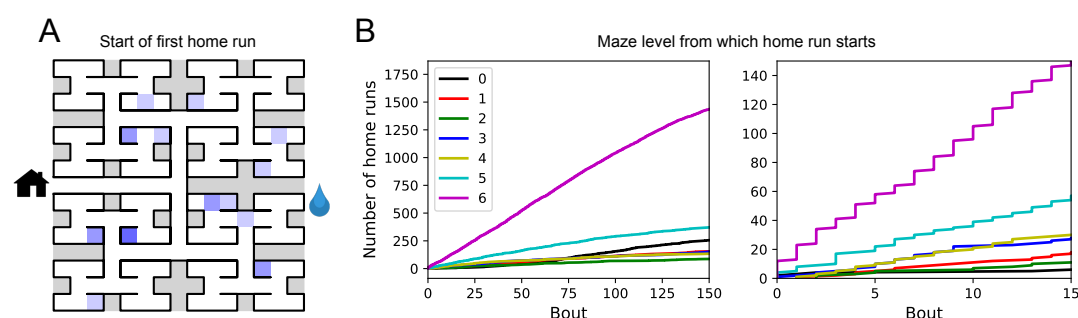


Figure 5. Homing succeeds on first attempt. (A) Locations in the maze where the 19 animals started their first return to the exit (home run). Some locations were used by 2 or 3 animals (darker color). (B) Left: The cumulative number of home runs from different levels in the maze, summed over all animals, and plotted against the bout number. Level 0 = first T-junction, level 6 = end nodes. Right: Zoom of (Left) into early bouts.

Figure 5–figure supplement 1. Entry paths do not retrace exit paths.

identified to a precision of ~200 s. We varied the criterion of performance by asking for even longer error-free paths, but the results were largely unchanged and no additional discontinuity appeared. These observations suggest that mice can acquire a complex decision-making skill rather suddenly. A mouse may have multiple moments of sudden insight that affect different aspects of its behavior. The exact time of the insight cannot be predicted but is easily identified post-hoc. Future neurophysiological studies of the phenomenon will face the interesting challenge of capturing these singular events.

One-shot learning of the home path

For an animal entering an unfamiliar environment, the most important path to keep in memory may be the escape route. In the present case that is the route to the maze entrance, from which the tunnel leads home to the cage. We expected that the mice would begin by penetrating into the maze gradually and return home repeatedly so as to confirm the escape route. This might help build a memory of the home path gradually level-by-level into the binary tree. Nothing could be further from the truth.

At the end of any given bout into the maze, there is a “home run”, namely the direct path without reversals that takes the animal to the exit (see *Figure 3–figure supplement 1*). *Figure 5A* shows the nodes where each animal started its first home run, following the first penetration into the maze. With few exceptions that first home run began from an end node, as deep into the maze as possible. Recall that this involves making the correct choice at six successive 3-way intersections, an outcome that is unlikely to happen by chance.

The above hypothesis regarding gradual practice of home runs would predict that short home runs should appear before long ones in the course of the experiment. The opposite is the case (*Figure 5B*). In fact, the end nodes (level 6 of the maze) are by far the favorite place from which to return to the exit, and those maximal-length home runs systematically appear before shorter ones. This conclusion was confirmed for each individual animal, whether rewarded or unrewarded.

Clearly the animals do not practice the home path or build it up gradually. Instead they seem to possess an Ariadne’s thread (*Pseudo-Apollodorus, 1st Century AD?*) starting with their first excursion into the maze, long before they might have acquired any general knowledge of the maze layout. On the other hand the mouse does not follow the strategy of Theseus, namely to precisely retrace the path that led it into the labyrinth. In that case the animal’s home path should be the reverse of the path into the maze that started the bout. Instead the entry path

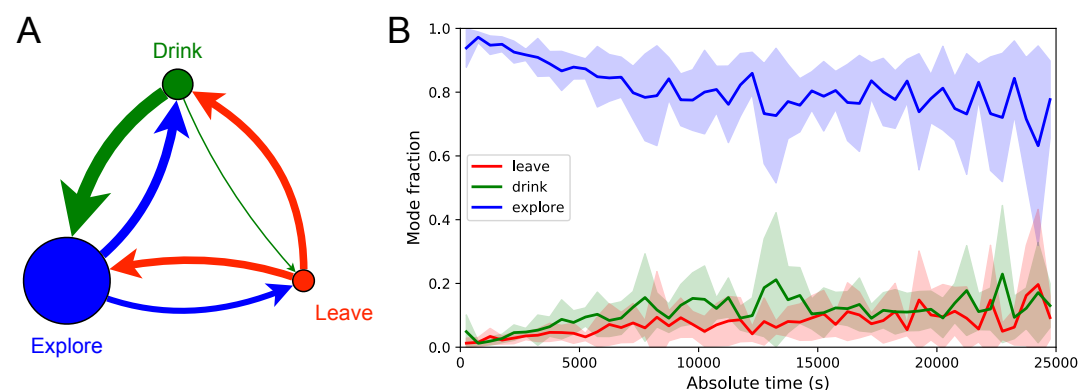


Figure 6. Exploration is a dominant and persistent mode of behavior. (A) Ethogram for rewarded animals. Area of the circle reflects the fraction of time spent in each behavioral mode averaged over animals and duration of the experiment. Width of the arrow reflects the probability of transitioning to another mode. ‘Drink’ involves travel to the water port and time spent there. Transitions from ‘Leave’ represent what the animal does at the start of the next bout into the maze. (B) The fraction of time spent in each mode as a function of absolute time throughout the night. Mean \pm SD across the 10 rewarded animals.

Figure 6–figure supplement 1. Three modes of behavior.

222 and the home path have very little overlap (*Figure 5–figure supplement 1*). It appears that the
223 animal acquires a homing strategy over the course of a single bout, and in a manner that allows
224 a direct return home from locations not previously encountered.

225 **Structure of behavior in the maze**

226 Here we focus on rules and patterns that govern the animal’s activity in the maze on both large
227 and small scales.

228 **Behavioral states**

229 Once the animal has learned to perform long uninterrupted paths to the water port, one can
230 categorize its behavior by three states: (1) walking to the water port; (2) walking to the exit;
231 and (3) exploring the maze. Operationally we define exploration as all periods in which the
232 animal is in the maze but not on a direct path to water or to the exit. For the ten sated animals
233 this includes all times in the maze except for the walks to the exit.

234 *Figure 6* illustrates the occupancies and transition probabilities between these states. The
235 animals spent most of their time by far in the exploration state: 84% for rewarded and 95%
236 for unrewarded mice. Across animals there was very little variation in the balance of the 3
237 modes (*Figure 6–figure supplement 1*). The rewarded mice began about half their bouts into
238 the maze with a trip to the water port and the other half by exploring (*Figure 6A*). After a
239 drink, the animals routinely continued exploring, about 90% of the time.

240 For water-deprived animals the dominance of exploration persisted even at a late stage of
241 the night when they routinely executed perfect exploitation bouts to and from the water port:
242 Over the duration of the night the ‘explore’ fraction dropped slightly from 0.92 to 0.75, with the
243 balance accrued to the ‘drink’ and ‘leave’ modes as the animals executed many direct runs to the
244 water port and back. The unrewarded group of animals also explored the maze throughout the
245 night even though it offered no overt rewards (*Figure 6–figure supplement 1*). One suspects
246 that the animals derive some intrinsic reward from the act of patrolling the environment itself.

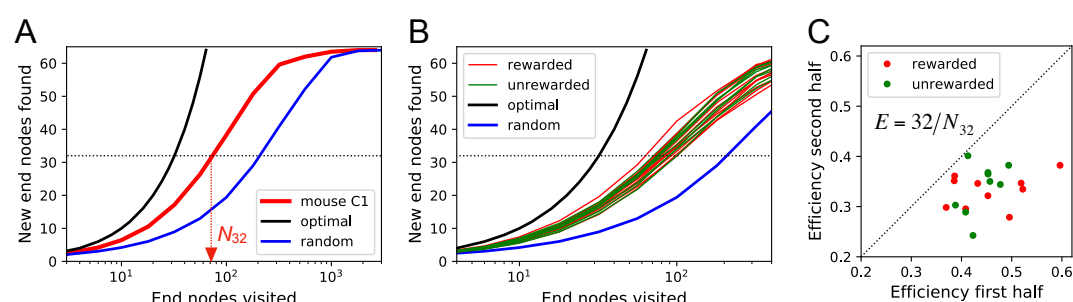


Figure 7. Exploration covers the maze efficiently. (A) The number of distinct end nodes encountered as a function of the number of end nodes visited for: mouse C1 (red); the optimal explorer agent (black); an unbiased random walk (blue). Arrowhead: the value $N_{32} = 76$ by which mouse C1 discovered half of the end nodes. (B) An expanded section of the graph in A including curves from 10 rewarded (red) and 9 unrewarded (green) animals. The efficiency of exploration, defined as $E = 32/N_{32}$, is 0.385 ± 0.050 (SD) for rewarded and 0.384 ± 0.039 (SD) for unrewarded mice. (C) The efficiency of exploration for the same animals, comparing the values in the first and second halves of the time in the maze. The decline is a factor of 0.74 ± 0.12 (SD) for rewarded and 0.81 ± 0.13 (SD) for unrewarded mice.

Figure 7—figure supplement 1. Efficiency of exploration

Efficiency of exploration

During the direct paths to water and to the exit the animal behaves deterministically, whereas the exploration behavior appears stochastic. Here we delve into the rules that govern the exploration component of behavior.

One can presume that a goal of the exploratory mode is to rapidly survey all parts of the environment for the appearance of new resources or threats. We will measure the efficiency of exploration by how rapidly the animal visits all end nodes of the binary maze, starting at any time during the experiment. The optimal agent with perfect memory and complete knowledge of the maze – including the absence of any loops – could visit the end nodes systematically one after another without repeats, thus encountering all of them after just 64 visits. A less perfect agent, on the other hand, will visit the same node repeatedly before having encountered all of them. *Figure 7A* plots for one exploring mouse the number of distinct end nodes it encountered as a function of the number of end nodes visited. The number of new nodes rises monotonically; 32 of the end nodes have been discovered after the mouse checked 76 times; then the curve gradually asymptotes to 64. We will characterize the efficiency of the search by the number of visits N_{32} required to survey half the end nodes, and define

$$E = \frac{32}{N_{32}}. \quad (1)$$

This mouse explores with efficiency $E = 32/76 = 0.42$. For comparison, *Figure 7A* plots the performance of the optimal agent ($E = 1.0$) and that of a random walker that makes random decisions at every 3-way junction ($E = 0.23$). Note the mouse is about half as efficient as the optimal agent, but twice as efficient as a random walker.

The different mice were remarkably alike in this component of their exploratory behavior (*Figure 7B*): across animals the efficiency varied by only 11% of the mean (0.387 ± 0.044 SD). Furthermore there was no detectable difference in efficiency between the rewarded animals and the sated unrewarded animals. Over the course of the night the efficiency declined significantly for almost every animal – whether rewarded or not – by an average of 23% (*Figure 7C*).

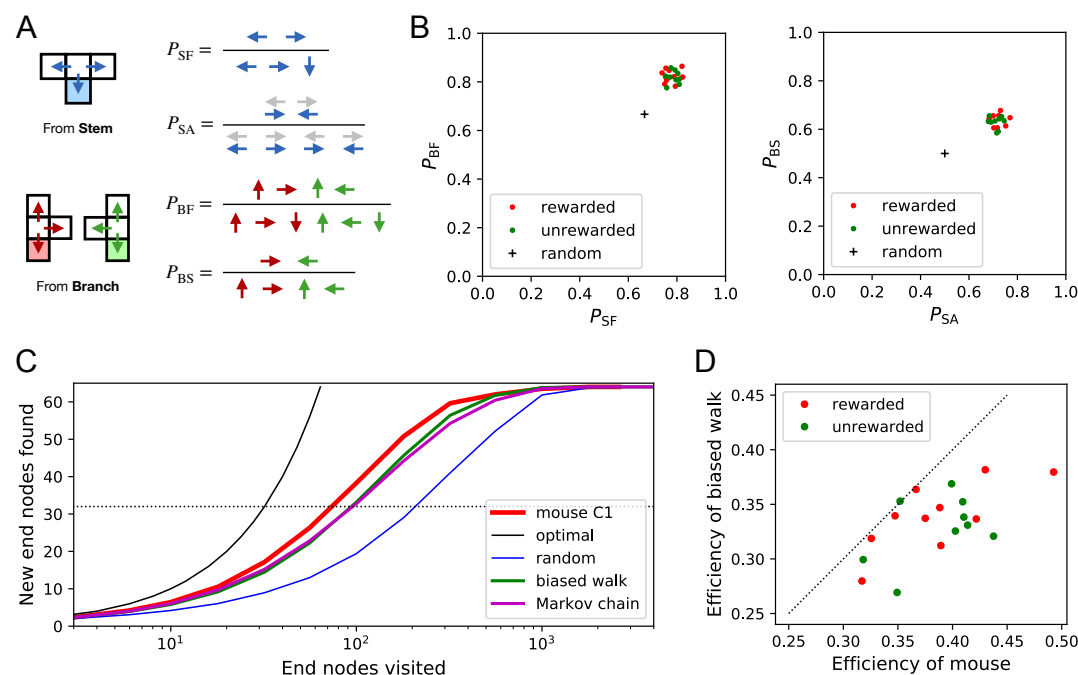


Figure 8. Turning biases favor exploration. (A) Definition of four turning biases at a T-junction based on the ratios of actions taken. Top: An animal arriving from the stem of the T (shaded) may either reverse or turn left or right. P_{SF} is the probability that it will move forward rather than reversing. Given that it moves forward, P_{SA} is the probability that it will take an alternating turn from the preceding one (gray), i.e. left-right or right-left. Bottom: An animal arriving from the bar of the T may either reverse or go straight, or turn into the stem of the T. P_{BF} is the probability that it will move forward through the junction rather than reversing. Given that it moves forward, P_{BS} is the probability that it turns into the stem. (B) Scatter graph of the biases P_{SF} and P_{BF} (left) and P_{SA} and P_{BS} (right). Every dot represents a mouse. Cross: values for an unbiased random walk. (C) Exploration curve of new end nodes discovered vs end nodes visited, displayed as in Figure 7A, including results from a biased random walk with the 4 turning biases derived from the same mouse, as well as a more elaborate Markov-chain model (see Figure 10C). (D) Efficiency of exploration (Equation 1) in 19 mice compared to the efficiency of the corresponding biased random walk.

Figure 8-figure supplement 1. Bias statistics.

Rules of exploration

What allows the mice to search much more efficiently than a random walking agent? We inspected more closely the decisions that the animals make at each 3-way junction. It emerged that these decisions are governed by strong biases (*Figure 8*). The probability of choosing each arm of a T-junction depends crucially on how the animal entered the junction. The animal can enter a T-junction from 3 places and exit it in 3 directions (*Figure 8A*). By tallying the frequency of all these occurrences across all T-junctions in the maze one finds clear deviations from an unbiased random walk (*Figure 8B*, *Figure 8-figure supplement 1*).

First, the animals have a strong preference for proceeding through a junction rather than returning to the preceding node (P_{SF} and P_{BF} in *Figure 8B*). Second there is a bias in favor of alternating turns left and right rather than repeating the same direction turn (P_{SA}). Finally, the mice have a mild preference for taking a branch off the straight corridor rather than proceeding straight (P_{BS}). A comparison across animals again revealed a remarkable degree of consistency even in these local rules of behavior: The turning biases varied by only 3% across the population and even between the rewarded and unrewarded groups (*Figure 8B*, *Figure 8-figure supplement 1*).

Qualitatively, one can see that these turning biases will improve the animal's search strategy. The forward biases P_{SF} and P_{BF} keep the animal from re-entering territory it has covered already. The bias P_{BS} favors taking a branch that leads out of the maze. This allows the animal to rapidly cross multiple levels during an outward path and then enter a different territory. By comparison, the unbiased random walk tends to get stuck in the tips of the tree and revisits the same end nodes many times before escaping. To test this intuition we simulated a biased random agent whose turning probabilities at a T-junction followed the same biases as measured from the animal (*Figure 8C*). These biased agents did in fact search with much higher efficiency than the unbiased random walk. They did not fully explain the behavior of the mice (*Figure 8D*), accounting for ~87% of the animal's efficiency (compared to 60% for the random walk). A more sophisticated model of the animal's behavior - involving many more parameters (*Figure 10C*) - failed to get any closer to the observed efficiency (*Figure 8C*, *Figure 7-figure supplement 1C*). Clearly some components of efficient search in these mice remain to be understood.

Systematic node preferences

A surprising aspect of the animals' explorations is that they visit certain end nodes of the binary tree much more frequently than others (*Figure 9*). This effect is large: more than a factor of 10 difference between the occupancy of the most popular and least popular end nodes (*Figure 9A-B*). This was surprising given our efforts to design the maze symmetrically, such that in principle all end nodes should be equivalent. Furthermore the node preferences were very consistent across animals and even across the rewarded and unrewarded groups. Note that the standard error across animals of each node's occupancy is much smaller than the differences between the nodes (*Figure 9B*).

The nodes on the periphery of the maze are systematically preferred. Comparing the outermost ring of 26 end nodes (excluding the water port and its neighbor) to the innermost 16 end nodes, the outer ones are favored by a large factor of 2.2. This may relate to earlier reports of a "centrifugal tendency" among rats patrolling a maze (*Uster et al., 1976*).

Interestingly, the biased random walk using four bias numbers (*Figure 8*, *Figure 10D*) replicates a good amount of the pattern of preferences. For unrewarded animals, where the maze symmetry is not disturbed by the water port, the biased random walk predicts 51% of the observed variance across nodes (*Figure 9C*), and an outer/inner node preference of 1.97, almost matching the observed ratio of 2.20. The far more complex Markov-chain model of behavior (*Figure 10C*) performed slightly better, explaining 66% of the variance in port visits

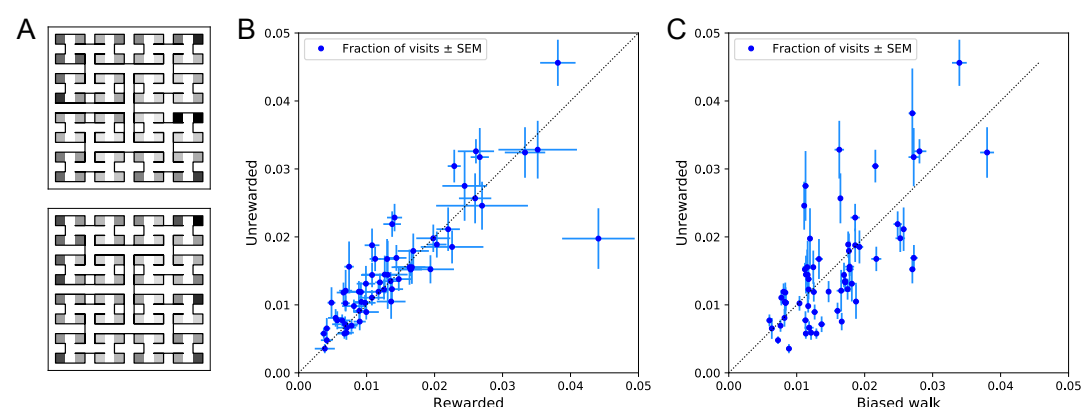


Figure 9. Preference for certain end nodes during exploration. (A) The number of visits to different end nodes encoded by a gray scale. Top: rewarded, bottom: unrewarded animals. Gray scale spans a factor of 12 (top) or 13 (bottom). (B) The fraction of visits to each end node, comparing the rewarded vs unrewarded group of animals. Each data point is for one end node, the error bar is the SEM across animals in the group. The outlier on the bottom right is the neighbor of the water port, a frequently visited end node among rewarded animals. The water port is off scale and not shown. (C) As in panel B but comparing the unrewarded animals to their simulated 4-bias random walks. These biases explain 51% of the variance in the observed preference for end nodes.

and matching the outer/inner node preference of 2.20.

Models of maze behavior

Moving beyond the efficiency of exploration one may ask more broadly: How well do we really understand what the mouse does in the maze? Can we predict its action at the next junction? Once the predictable component is removed, how much intrinsic randomness remains in the mouse's behavior? Here we address these questions using more sophisticated models that predict the probability of the mouse's future actions based on the history of its trajectory.

At a formal level, the mouse's trajectory through the maze is a string of numbers standing for the nodes the animal visited (*Figure 10A* and *Figure 3-figure supplement 1*). We want to predict the next action of the mouse, namely the step that takes it to the next node. The quality of the model will be assessed by the cross-entropy between the model's predictions and the mouse's observed actions, measured in bits per action. This is the uncertainty that remains about the mouse's next action given the prediction from the model. The ultimate lower limit is the true source entropy of the mouse, namely that component of its decisions that cannot be explained by the history of its actions.

One family of models we considered are fixed-depth Markov chains (*Figure 10B*). Here the probability of the next action a_{t+1} is specified as a function of the history stretching over the k preceding nodes (s_{t-k+1}, \dots, s_t) . In fitting the model to the mouse's actual node sequence one tallies how often each history leads to each action, and uses those counts to estimate the conditional probabilities $p(a_{t+1}|s_{t-k+1}, \dots, s_t)$. Given a new node sequence, the model will then use the history strings (s_{t-k+1}, \dots, s_t) to predict the outcome of the next action. In practice we trained the model on 80% of the animal's trajectory and tested it by evaluating the cross-entropy on the remaining 20%.

Ideally, the depth k of these action trees would be very large, so as to take as much of the prior history into account as possible. However, one soon runs into a problem of over-fitting: Because each T-junction in the maze has 3 neighboring junctions, the number of possible histories grows as 3^k . As k increases, this quickly exceeds the length of the measured node sequence, so that every history appears only zero or one times in the data. At this point one

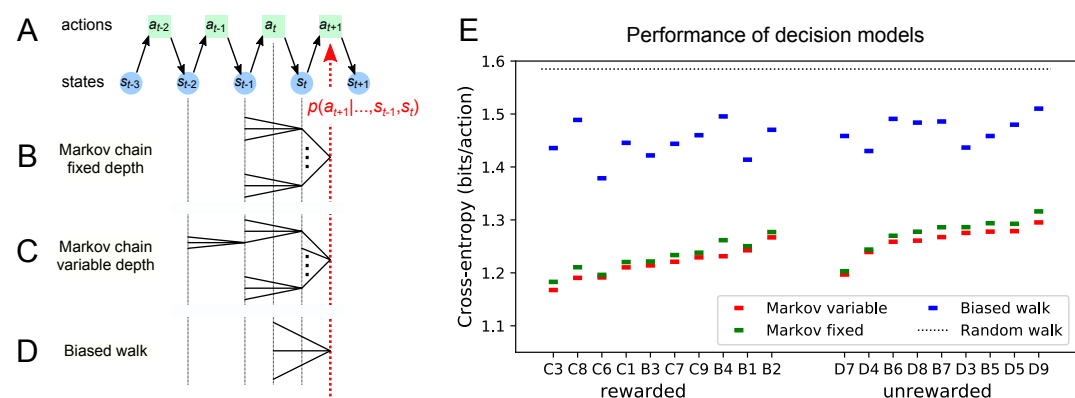


Figure 10. Recent history constrains the mouse's decisions. (A) The mouse's trajectory through the maze produces a sequence of states s_t = node occupied after step t . From each state, up to 3 possible actions lead to the next state (end nodes allow only one action). We want to predict the animal's next action, a_{t+1} , based on the prior history of states or actions. (B-D) Three possible models to make such a prediction. (B) A fixed-depth Markov chain where the probability of the next action depends only on the current state s_t and the preceding state s_{t-1} . The branches of the tree represent all 3×127 possible histories (s_{t-1}, s_t) . (C) A variable-depth Markov chain where only certain branches of the tree of histories contribute to the action probability. Here one history contains only the current state, some others reach back three steps. (D) A biased random walk model, as defined in *Figure 8*, in which the probability of the next action depends only on the preceding action, not on the state. (E) Performance of the models in (B,C,D) when predicting the decisions of the animal at T-junctions. In each case we show the cross-entropy between the predicted action probability and the real actions of the animal (lower values indicate better prediction, perfect prediction would produce zero). Dotted line represents an unbiased random walk with 1/3 probability of each action.

Figure 10-figure supplement 1. Markov model fits.

can no longer estimate any probabilities, and cross-validation on a different segment of data fails catastrophically. In practice we found that this limitation sets in already beyond $k = 2$ (Figure 10–figure supplement 1A). To address this issue of data-limitation we developed a variable-depth Markov chain (Figure 10C). This model retains longer histories, but only if they occur frequently enough to allow a reliable probability estimate (see Methods, Figure 10–figure supplement 1B–C). In addition, we explored different schemes of pooling the counts across certain T-junctions that are related by the symmetry of the maze (see Methods).

With these methods we focused on the portions of trajectory when the mouse was in ‘explore’ mode, because the segments in ‘drink’ and ‘leave’ mode are fully predictable. Furthermore, we evaluated the models only at nodes corresponding to T-junctions, because the decision from an end node is again fully predictable. Figure 10E compares the performance of various models of mouse behavior. The variable-depth Markov chains routinely produced the best fits, although the improvement over fixed-depth models was modest. Across all 19 animals in this study the remaining uncertainty about the animal’s action at a T-junction is 1.237 ± 0.035 (SD) bits/action, compared to the prior uncertainty of $\log_2 3 = 1.585$ bits. The rewarded animals have slightly lower entropy than the unrewarded ones (1.216 vs 1.261 bits/action). The Markov chain models that produced the best fits to the behavior used history strings with an average length of ~ 4 .

We also evaluated the predictions obtained from the simple biased random walk model (Figure 10D). Recall that this attempts to capture the history-dependence with just 4 bias parameters (Figure 8A). As expected this produced considerably higher cross-entropies than the more sophisticated Markov chains (by about 18%, Figure 10E). Finally we used several professional file compression routines to try and compress the mouse’s node sequence. In principle, this sets an upper bound on the true source entropy of the mouse, even if the compression algorithm has no understanding of animal behavior. The best such algorithm (bzip2 compression (Seward, 2019)) far under-performed all the other models of mouse behavior, giving 43% higher cross-entropy on average, and thus offered no additional useful bounds.

We conclude that during exploration of the maze the mouse’s choice behavior is strongly influenced by its current location and ~ 3 locations preceding it. There are minor contributions from states further back. By knowing the animal’s history one can narrow down its action plan at a junction from the *a priori* 1.59 bits (one of three possible actions) to just ~ 1.24 bits. This finally is a quantitative answer to the question, “How well can one predict the animal’s behavior?” Whether the remainder represents an irreducible uncertainty – akin to “free will” of the mouse – remains to be seen. Readers are encouraged to improve on this number by applying their own models of behavior to our published data set.

Discussion

Summary of contributions

We present a new approach to the study of learning and decision-making in mice. We give the animal access to a complex labyrinth and leave it undisturbed for a night while monitoring its movements. The result is a rich data set that reveals new aspects of learning and the structure of exploratory behavior. With these methods we find that mice learn a complex task that requires 6 correct 3-way decisions after only ~ 10 experiences of success (Figure 2, Figure 3). Along the way the animal gains task knowledge in discontinuous steps that can be localized to within a few minutes of resolution (Figure 4). Underlying the learning process is an exploratory behavior that occupies 90% of the animal’s time in the maze, persists long after the task has been mastered, and even in complete absence of an extrinsic reward (Figure 6). The decisions the animal makes at choice points in the labyrinth are constrained in part by

the history of its actions (*Figure 8, Figure 10*), in a way that favors efficient searching of the maze (*Figure 7*). This microstructure of behavior is surprisingly consistent across mice, with variation in parameters of only a few percent (*Figure 8*). Our most expressive models to predict the animal's choices still leave a remaining uncertainty of ~1.24 bits per decision (*Figure 10*), a quantitative benchmark by which competing models can be tested. Finally – as discussed below – some of the observations constrain what algorithms the animals might use for learning and navigation.

Historical context

Mazes have been a staple of animal psychology for well over 100 years. The early versions were true labyrinths. For example, *Small (1901)* built a model of the maze in Hampton Court gardens scaled to rat size. Subsequent researchers felt less constrained by Victorian landscapes and began to simplify the maze concept. Most commonly the maze offered one standard path from a starting location to a food reward box. A few blind alleys would branch from the standard path, and researchers would tally how many errors the animal committed by briefly turning into a blind (*Tolman and Honzik, 1930*). Later on, the design was further reduced to a single T-junction. After all, the elementary act of maze navigation is whether to turn left or right at a junction (*Tolman, 1938*), so why not study that process in isolation? One can avoid the tedium of carrying the animal from the exit to the entrance by closing off all branches of the T, forcing the animal to retrace its steps, which leads to the W-track (*Kim and Frank, 2009*). And reducing the concept even further, one can ask the animal to refrain from walking altogether, and instead poke its nose into a hole on the left or the right side of a box (*Uchida and Mainen, 2003*). This led to the popular behavior boxes now found in rodent neuroscience laboratories everywhere. While each of these reductions of the “maze” concept enabled a new type of experiment, the essence of a “confusing network of paths” has been lost entirely, and with it the behavioral richness of the animals navigating those paths.

On this background our experimental design is a step back to complex labyrinths, enhanced with fully automated animal tracking and new methods of data analysis. In fact, our labyrinth is considerably more complex than Hampton Court or most of the mazes employed by Tolman and others (*Tolman and Honzik, 1930; Buel, 1934; Munn, 1950a*): The blind alleys in those mazes are all short and unbranched. When an animal strays from the target path it receives feedback quickly and can correct. By contrast our binary tree maze has 64 equally deep branches, only one of which contains the reward port. If the animal makes a mistake at any level of the tree it can find out only after traveling all the way to the last node.

Another unusual but crucial aspect of our experimental design is the absence of any human interference. Most studies of animal navigation and learning involve some kind of trial structure. For example the experimenter puts the rat in the start box, watches it make its way through the maze, coaxes it back on the path if necessary, and picks it up once it reaches the target box. Then another trial starts. In modern experiments with two-alternative-forced-choice (2AFC) behavior boxes the animal doesn't have to be picked up, but a trial starts with appearance of a cue, and then proceeds through some strict protocol through delivery of the reward. The argument in favor of imposing a trial structure is that it creates reproducible conditions, so that one can gather comparable data and average them suitably over many trials.

Our experiments had no imposed structure whatsoever; in fact it may be inappropriate to call them experiments. The investigator opened the entry to the maze in the evening and did not return until the morning. A potential advantage of leaving the animals to themselves is that they are more likely to engage in mouse-like behavior, rather than constantly responding to the stress of human interference or the pressures from being a cog in a behavior machine. The result was a rich data set, with the typical animal delivering ~15,000 decisions in a single

night, even if one only counts the nodes of the binary tree as decision points. Since the mice made all the choices, the scientific effort lay primarily in adapting methods of data analysis to the nature of mouse trajectories. Somewhat surprisingly, the absence of experimental structure was no obstacle to making precise and reproducible measurements of the animal's behavior.

How fast do animals learn?

Among the wide range of phenomena of animal learning, one can distinguish easy and hard tasks by some measure of task complexity. In a simple picture of a behavioral task the animal needs to recognize several different contexts and based on that express one of several different actions. One can draw up a contingency table between contexts and actions, and measure the complexity of the task by the mutual information in that table. This ignores any task difficulties associated with sensing the context at all or with producing the desired actions. However, in all the examples discussed here the stimuli are discriminated easily and the actions come naturally, thus the learning difficulty lies only in forming the associations, not in sharpening the perceptual mechanisms or practicing complex motor output.

Many well-studied behaviors have a complexity of 1 bit or less, and often animals can learn these associations after a single experience. For example, the Bruce effect (*Bruce, 1959*) is a learning phenomenon in which the female mouse forms an olfactory memory of her mate. This allows her to identify a foreign male in a subsequent encounter, in which case she aborts the pregnancy. In effect the female maps two different contexts (smell of mate vs non-mate) onto two kinds of pregnancy outcomes (carry to term vs abort). The mutual information in that contingency table is at most 1 bit, and may be considerably lower, for example if non-mate males are very rare or very frequent. Mice form the correct association after a single instance of mating, although proper memory formation requires several hours of exposure to the mate odor (*Rosser and Keverne, 1985*).

Similarly fear learning under the common electroshock paradigm establishes a mapping between two kinds of contexts (paired with shock vs innocuous) and two actions (freeze vs proceed), again with an upper bound of 1 bit of complexity. Rats and mice will form the association after a single experience lasting only seconds, and alter their behavior over several hours (*Fanselow and Bolles, 1979; Bourchuladze et al., 1994*). This is an adaptive warning system to deal with life-threatening events, and rapid learning here has a clear survival value.

Animals are particularly adept at learning a new association between an odor and food. For example bees will extend their proboscis in response to a new odor after just one pairing trial where the odor appeared together with sugar (*Bitterman et al., 1983*). Similarly rodents will start digging for food in a scented bowl after just a few pairings with that odor (*Cleland et al., 2009*). Again, these are 1-bit tasks learned rapidly after one or a few experiences.

By comparison the tasks that a mouse performs in the labyrinth are more complex. For example, the path from the maze entrance to the water port involves 6 junctions, each with 3 options. At a minimum 6 different contexts must be mapped correctly into one of 3 actions each, which involves $6 \cdot \log_2 3 = 9.5$ bits of complexity. The animals begin to execute perfect paths from the entrance to the water port well within the first hour (*Figure 2C, Figure 3B*). At a later stage during the night the animal learns to walk direct paths to water from many different locations in the maze (*Figure 4*); by this time it has consumed 10-20 rewards. In the limit, if the animal could turn correctly towards water from each of 63 junctions in the maze, it would have learned $63 \cdot \log_2 3 = 100$ bits. Conservatively we estimate that the animals have mastered 10-20 bits of complexity based on 10-20 reward experiences within an hour of time spent in the maze. Note this considers only information about the water port and ignores whatever else the animals are learning about the maze during their incessant exploratory forays. These numbers align well with classic experiments on rats in diverse mazes and problem boxes

491 *Munn (1950a)*. Although those tasks come in many varieties, a common theme is that ~10
492 successful trials are sufficient to learn ~10 decisions (*Woodrow, 1942*).

493 In a different corner of the speed-complexity space are the many 2-alternative-forced-choice
494 (2AFC) tasks in popular use today. These tend to be 1-bit tasks, for example the monkey should
495 flick its eyes to the left when visual motion is to the left (*Newsome and Pare, 1988*), or the
496 mouse should turn a steering wheel to the right when a light appears on the left (*Burgess et al.,*
497 *2017*). Yet the animals take a long time to learn these simple tasks. For example, the mouse
498 with the steering wheel requires about 10,000 experiences before performance saturates. It
499 never gets particularly good, with a typical hit rate only 2/3 of the way from random to perfect.
500 All this training takes 3-6 weeks; in the case of monkeys several months. The rate of learning,
501 measured in task complexity per unit time, is surprisingly low: < 1 bit/month compared to ~10
502 bits/h observed in the labyrinth. The difference is a factor of 6,000. Similarly when measured
503 in complexity learned per reward experience: The 2AFC mouse may need 5,000 rewards to
504 learn a contingency table with 1 bit complexity, the mouse in the maze needs ~10 rewards to
505 learn 10 bits. Given these differences in learning rate spanning many orders of magnitude,
506 it seems likely that whatever neural process underlies ultra-slow 2AFC learning is different
507 from the implementation of fast learning in the labyrinth and other complex environments.
508 Furthermore, the ultra-slow mode of learning may have little relevance for an animal's natural
509 condition. In the month that the 2AFC mouse requires to finally report the location of a light,
510 its relative in the wild has developed from a baby to having its own babies. Along the way, that
511 wild mouse had to make many decisions, often involving high stakes, without the benefit of
512 10,000 trials of practice.

513 **Sudden insight**

514 The dynamics of the learning process are often conceived as a continuously growing associ-
515 ation between stimuli and actions, with each reinforcing experience making an infinitesimal
516 contribution. The reality can be quite different. When a child first learns to balance on a bicycle,
517 performance goes from abysmal to astounding within a few seconds. The timing of such a
518 discontinuous step in performance seems impossible to predict but easy to recognize after the
519 fact.

520 From the early days of animal learning experiments there have been warnings against the
521 tendency to average learning curves across subjects (*Krechevsky, 1932; Estes, 1956*). The
522 average of many discontinuous curves will certainly look continuous and incremental, but that
523 reassuring shape may miss the essence of the learning process. A recent reanalysis of many
524 Pavlovian conditioning experiments suggested that discontinuous steps in performance are the
525 rule rather than the exception (*Gallistel et al., 2004*). Here we found that the same applies to
526 navigation in a complex labyrinth. While the average learning curve presents like a continuous
527 function (*Figure 3B*), the individual records of water rewards show that each animal improves
528 rather quickly but at different times (*Figure 3A*).

529 Owing to the unstructured nature of the experiment, the mouse may adopt different policies
530 for getting to the water port. In at least half the animals we observed a discontinuous change
531 in that policy, namely when the animal started using efficient direct paths within the maze
532 (*Figure 4, Figure 4-figure supplement 2*). This second switch happened considerably after
533 the animal started collecting rewards, and did not greatly affect the reward rate. Furthermore,
534 the animals never reverted to the less efficient policy, just as a child rarely unlearns to balance
535 a bicycle.

536 Presumably this switch in performance reflects some discontinuous change in the animal's
537 internal model of the maze, what Tolman called the "cognitive map" (*Tolman, 1948; Behrens*
538 *et al., 2018*). In the unrewarded animals we could not detect any discontinuous change in the

539 use of long paths. However, as Tolman argued, those animals may well acquire a sophisticated
540 cognitive map that reveals itself only when presented with a concrete task, like finding water.
541 Future experiments will need to address this. The discontinuous changes in performance pose
542 a challenge to conventional models of reinforcement learning, in which reward events are the
543 primary driver of learning and each event contributes an infinitesimal update to the action
544 policy. It will also be important to model the acquisition of distinct kinds of knowledge that
545 contribute to the same behavior, like the location of the target and efficient routes to approach
546 it.

547 **Exploratory behavior**

548 By all accounts the animals spent a large fraction of the night exploring the maze (*Figure 1–*
549 *figure supplement 2*). The water-deprived animals continued their forays into the depths of
550 the maze long after they had found the water port and learned to exploit it regularly. The sated
551 animals experienced no overt reward from the maze, yet they likewise spent nearly half their
552 time in that environment. As has been noted many times, animals – like humans – derive some
553 form of intrinsic reward from exploration (*Berlyne, 1960*). Some have suggested that there
554 exists a homeostatic drive akin to hunger and thirst that elicits the information-seeking activity,
555 and that the drive is in turn sated by the act of exploration (*Hughes, 1997*). If this were the
556 case, then the drive to explore should be weakest just after an episode of exploration, much as
557 the drive for food-seeking is weaker after a big meal.

558 Our observations are in conflict with this notion. The animal is most likely to enter the maze
559 within the first minute of its return to the cage (*Figure 1–figure supplement 3*), a strong trend
560 that runs opposite to the prediction from satiation of curiosity. Several possible explanations
561 come to mind: (1) On these very brief visits to the cage the animal may just want to certify
562 that the exit route to the safe environment still exists, before continuing with exploration of the
563 maze. (2) The temporal contrast between the boredom of the cage and the mystery of the maze
564 is highest right at the moment of exit from the maze, and that may exert pressure to re-enter the
565 maze. Understanding this in more detail will require dedicated experiments. For example, one
566 could deliberately deprive the animals of access to the maze for some hours, and test whether
567 that results in an increased drive to explore, as observed for other homeostatic drives around
568 eating, drinking, and sleeping.

569 When left to their own devices, mice choose to spend much of their time engaged in
570 exploration. In the maze, mice follow the collection of a water drop with a bout of exploration
571 90% of the time (*Figure 6B*). One wonders how that affects their actions when they are strapped
572 into a rigid behavior machine, like a 2AFC choice box. Presumably the drive to explore persists,
573 perhaps more so because the forced environment is so unpleasant. And within the confines
574 of the two alternatives, the only act of exploration the mouse has left is to give the wrong
575 answer. This would manifest as an unexpectedly high error rate on unambiguous stimuli,
576 sometimes called the “lapse rate” (*Carandini and Churchland, 2013*). The fact that the lapse
577 rate decreases only gradually over weeks to months of training (*Burgess et al., 2017*) suggests
578 that it is difficult to crush the animal’s drive to explore.

579 The animals in our experiments had never been presented with a maze environment, yet they
580 quickly settled into a steady mode of exploration. Once a mouse progressed beyond the first
581 intersection it typically entered deep into the maze to one or more end nodes (*Figure 5*). Within
582 50 s of the first entry the animals adopted a steady speed of locomotion that they would retain
583 throughout the night (*Figure 2–figure supplement 1*). Within 250 s of first contact with the
584 maze the average animal already spent 50% of its time there (*Figure 1–figure supplement 2*).
585 Contrast this with a recent study of “free exploration” in an exposed arena: Those animals
586 required several hours before they even completed one walk around the perimeter (*Fonio et al.,*

2009). Here the drive to explore is clearly pitted against fear of the open space, which may not be conducive to observing exploration *per se*.

The persistence of exploration throughout the entire duration of the experiment suggests that the animals are continuously surveying the environment, perhaps expecting new features to arise. These surveys are quite efficient: The animals cover all parts of the maze much faster than expected from a random walk (*Figure 7*). Effectively they avoid re-entering territory they surveyed just recently. It is often assumed that this requires some global memory of places visited in the environment (*Nagy et al., 2020; Olton, 1979*). Such memory would have to persist for a long time: Surveying half of the available end nodes typically required 450 turning decisions. However, we found that a global long-term memory is not needed to explain the efficient search. The animals seem to be governed by a set of local turning biases that require memory only of the most recent decision and no knowledge of location (*Figure 8*). These local biases alone can explain most of the character of exploration without any global understanding or long-term memory. Incidentally, they also explain other seemingly global aspects of the behavior, for example the systematic preference that the mice have for the outer rather than the inner regions of the maze (*Figure 9*). Of course, this argument does not exclude the presence of a long-term memory, which may reveal itself in some other feature of the behavior.

Perhaps the most remarkable aspect of these biases is how similar they are across all 19 mice studied here, regardless of whether the animal experienced water rewards or not (*Figure 8B, Figure 8-figure supplement 1*), and independent of the sex of the mouse. The four decision probabilities were identical across individuals to within a standard deviation of <0.03 . We cannot think of a trivial reason why this should be so. For example the two biases for forward motion (*Figure 8B left*) are poised halfway between the value for a random walk ($p = 2/3$) and certainty ($p = 1$). At either of those extremes, simple saturation might lead to a reproducible value, but not in the middle of the range. Why do different animals follow the exact same decision rules at an intersection between tunnels? Given that tunnel systems are part of the mouse's natural ecology, it is possible that those rules are innate and determined genetically. Indeed the rules by which mice build tunnels have a strong genetic component (*Weber et al., 2013*), so the rules for using tunnels may be written in the genes as well. The high precision with which one can measure those behaviors even in a single night of activity opens the way to efficient comparisons across genotypes, and also across animals with different developmental experience.

Finally, after mice discover the water port and learn to access it from many different points in the maze (*Figure 4*) they are presumably eager to discover other things. In ongoing work we installed three water ports (visible in the videos accompanying this article) and implemented a rule that activates the three ports in a cyclic sequence. Mice discovered all three ports rapidly and learned to visit them in the correct order. Future experiments will have to raise the bar on what the mice are expected to learn in a night.

Mechanisms of navigation

How do the animals navigate when they perform direct paths to the water port or to the exit? This question will require future directed experiments, but we can exclude a few candidate explanations based on observations so far. Early workers already concluded that rodents in a maze will use whatever sensory cues and tricks are available to accomplish their tasks (*Munn, 1950b*). Our maze was designed to restrict those options somewhat.

To limit the opportunity for visual navigation, the floor and walls of the maze are visually opaque. The ceiling is transparent, but the room is kept dark except for infrared illuminators. Even if the animal finds enough light, the goals (water port or exit) are invisible within the maze except from the immediately adjacent corridor. There are no visible beacons that would

635 identify the goal.

636 With regard to the sense of touch and kinesthetics, the maze was constructed for maximal
637 symmetry. At each level of the binary tree all the junctions have locally identical geometry,
638 with intersecting corridors of the same length. In practice the animals may well detect some
639 inadvertent cues, like an unusual drop of glue, that could identify one node from another.

640 The role of odors deserves particular attention because the mouse may use them both
641 passively and actively. Does the animal first find the water port by following the smell of water?
642 Probably not. For one, the port only emits a single drop of water when triggered by a nose
643 poke. Second, we observed many instances where the animal is in the final corridor adjacent to
644 the water port yet fails to discover it. The initial discovery seems to occur via touch. Finally, in
645 exploratory experiments with a different labyrinth we used an open bowl of water as a reward;
646 the correct path required traveling away from the water for many turns. The mice discovered
647 this path readily.

648 Do the animals lay down an odor trail to mark the location of the water port? This could
649 be a simple algorithm for externalized cognition: After finding a location to which you want
650 to return, urinate on the floor on the way back, gradually reducing the emissions along the
651 way. This would establish an odor gradient that you can follow uphill on the next foray. Taking
652 advantage of the symmetric layout of the maze, we rotated the entire maze by 180 degrees
653 between one foray and the next, while leaving both the entrance and the water port in the
654 same absolute location. Following that rotation the animal did in fact make a few visits to the
655 rotated port location, but then quickly exploited the real water port again, without any apparent
656 re-learning. Through further experiments of this type one can hope to test not only the role of
657 odor tracks, but also that of inadvertent construction details that might identify each node.

658 Finally we considered an algorithm that is often invoked for animals moving in an open
659 arena: vector-based navigation (*Wehner et al., 1996*). Once the animal discovers a target, it
660 keeps track of that target's heading and distance using a path integrator. When it needs to return
661 to the target it follows the heading vector and updates heading and distance until it arrives. This
662 is clearly not what the mice do in the labyrinth, as seen most easily by considering the "home
663 runs" back to the exit at the end of a bout. Here the target, namely the exit, is known from
664 the start of the bout, because the animal enters through the same hole. At the end of the bout,
665 when the mouse decides to exit from the maze, does it follow the heading vector to the exit?
666 *Figure 5A* shows the 13 locations from which mice returned in a direct path to the exit on their
667 very first foray. None of these locations is compatible with heading-based navigation: In each
668 case an animal following the heading to the exit would get stuck in a different end node first.

669 Future directed experiments will serve to further exclude candidate mechanisms of naviga-
670 tion. Since the animals normally solve the task within an hour, one can test a new hypothesis
671 quite efficiently. Understanding what mechanisms they use will then inform thinking about the
672 algorithm for learning, and about the neuronal mechanisms that implement it.

Methods and Materials

Experimental design

The goal of the study was to observe mice as they explored a complex environment for the first time, with little or no human interference and no specific instructions. In preliminary experiments we tested several labyrinth designs and water reward schedules. Eventually we settled on the protocol described here, and tested 20 mice in rapid succession. Each mouse was observed only over a 7-hour period during the first night it encountered the labyrinth.

Maze construction

The maze measured ~24 x 24 x 2 inches; for manufacture we used materials specified in inches, so dimensions are quoted in those non-SI units where appropriate. The ceiling was made of 0.5 inch clear acrylic. Slots of 1/8 inch width were cut into this plate on a 1.5 inch grid. Pegged walls made of 1/8 inch infrared-transmitting acrylic (opaque in the visible spectrum, ePlastics) were inserted into these slots and secured with a small amount of hot glue. The floor was a sheet of infrared-transmitting acrylic, supported by a thicker sheet of clear acrylic. The resulting corridors (1-1/8 inches wide) formed a 6-level binary tree with T-junctions and progressive shortening of each branch, ranging from ~12 inch to 1.5 inch (*Figure 1* and *Figure 2*). A single end node contained a 1.5 cm circular opening with a water delivery port (described below). The maze included provision for two additional water ports not used in the present report. In unrewarded experiments the water port was covered with an acrylic plate. Once per week the maze was submerged in cage cleaning solution. Between different animals the floor and walls were cleaned with ethanol.

Reward delivery system

The water reward port was controlled by a Matlab script on the main computer through an interface (Sanworks Bpod State Machine r1). Rewards were triggered when the animal's nose broke the IR beam in the water port (Sanworks Port interface + valve). The interface briefly opened the water valve to deliver ~30 μ L of water and flashed an infrared LED mounted outside the maze for 1 s. This served to mark reward events on the video recording. Following each reward, the system entered a time-out period for 90 s, during which the port did not provide further reward.

Cage and connecting passage

The entrance to the maze was connected to an otherwise normal mouse cage by red plastic tubing (3 cm dia, 1 m long). The cage contained food, bedding, nesting material, and in the case of unrewarded experiments also a normal water bottle.

Animals and treatments

All mice were C57Bl6/J animals (Jackson Labs) between the ages of 45 and 98 days (mean 62 days). Both sexes were used: 4 males and 6 females in the rewarded experiments, 5 males and 4 females in the unrewarded experiments. For water deprivation, the animal was transferred from its home cage (generally group-housed) to the maze cage ~22 h before the start of the experiment. Non-deprived animals were transferred minutes before the start. All procedures were performed in accordance with institutional guidelines and approved by the Caltech IACUC.

Video recording

All data reported here were collected over the course of 7 hours during the dark portion of the animal's light cycle. Video recording was initiated a few seconds prior to connecting the tunnel to the maze. Videos were recorded by an OpenCV python script controlling a single

717 webcam (Logitech C920) located ~1 m below the floor of the maze. The maze and access tube
718 were illuminated by multiple infrared LED arrays (center wavelength 850 nm). Three of these
719 lights illuminated the maze from below at a 45 degree angle, producing contrast to resolve
720 the animal's foot pads. The remaining lights pointed at the ceiling of the room to produce
721 backlight for a sharp outline of the animal.

722 **Animal tracking**

723 A version of DeepLabCut (*Nath et al., 2019*) modified to support gray-scale processing was
724 used to track the animal's trajectory, using key points at the nose, feet, tail base and mid-body.
725 All subsequent analysis was based on the trajectory of the animal's nose, consisting of positions
726 $x(t)$ and $y(t)$ in every video frame.

727 **Rates of transition between cage and maze**

728 This section relates to *Figure 1-figure supplement 3*. We entertained the hypothesis that the
729 animals become "thirsty for exploration" as they spend more time in the cage. In that case one
730 would predict that the probability of entering the maze in the next second will increase with
731 time spent in the cage. One can compute this probability from the distribution of residency
732 times in the cage, as follows:

733 Say $t = 0$ when the animal enters the cage. The probability density that the animal will
734 next leave the cage at time t is

$$p(t) = e^{-\int_0^t r(t') dt'} r(t) \quad (2)$$

735 where $r(t)$ is the instantaneous rate for entering the maze. So

$$\int_0^t p(t') dt' = 1 - e^{-\int_0^t r(t') dt'} \quad (3)$$

$$\int_0^t r(t') dt' = -\ln \left(1 - \int_0^t p(t') dt' \right) \quad (4)$$

736 This relates the cumulative of the instantaneous rate function to the cumulative of the
737 observed transition times. In this way we computed the rates

$$r_m(t) = \text{rate of entry into the maze as a function of time spent in the cage} \quad (5)$$

$$r_c(t) = \text{rate of entry into the cage as a function of time spent in the maze} \quad (6)$$

738 The rate of entering the maze is highest at short times in the cage (*Figure 1-figure supplement 3A*). It peaks after ~15 s in the cage and then declines gradually by a factor of 4 over
739 the first minute. So the mouse is most likely to enter the maze just after it returns from there.
740 This runs opposite to the expectation from a homeostatic drive for exploration, which should
741 be sated right after the animal returns. We found no evidence for an increase in the rate at
742 late times. These effects were very similar in rewarded and unrewarded groups and in fact the
743 tendency to return early was seen in every animal.

744 By contrast the rate of exiting the maze is almost perfectly constant over time (*Figure 1-figure supplement 3B*). In other words the exit from the maze appears like a constant rate

Poisson process. There is a slight elevation of the rate at short times among rewarded animals (*Figure 1-figure supplement 3B* top). This may come from the occasional brief water runs they perform. Another strange deviation is an unusual number of very short bouts (duration 2-12 s) among unrewarded animals (*Figure 1-figure supplement 3B* bottom). These are brief excursions in which the animal runs to the central junction, turns around, and runs to the exit. Several animals exhibited these, often several bouts in a row, and at all times of the night.

Reduced trajectories

From the raw nose trajectory we computed two reduced versions. First we divided the maze into discrete “cells”, namely the squares the width of a corridor that make up the grid of the maze. At any given time the nose is in one of these cells and that time series defines the **cell trajectory**.

At a coarser level still one can ask when the animal passes through the nodes of the binary tree, which are the decision points in the maze. The special cells that correspond to the nodes of the tree are those at the center of a T-junction and those at the leaves of the tree. We marked all the times when the trajectory $(x(t), y(t))$ entered a new node cell. If the animal leaves a node cell and returns to it before entering a different node cell, that is not considered a new node. This procedure defines a discrete **node sequence** s_i and corresponding arrival times at those nodes t_i . We call the transition between two nodes a “step”. Much of the analysis in this paper is derived from the animal’s node sequence. The median mouse performed 16,192 steps in the 7 h period of observation (mean = 15,257; SD = 3,340).

In *Figure 4* and *Figure 5* we count the occurrence of **direct paths** leading to the water port (a “water run”) or to the exit (a “home run”). A direct path is a node sequence without any reversals. *Figure 3-figure supplement 1* illustrates some examples.

If the animal makes one wrong step from the direct path, that step needs to be backtracked, adding a total of two steps to the length of the path. If further errors occur during backtracking they need to be corrected as well. The binary maze contains no loops, so the number of errors is directly related to the length of the path:

$$\text{Errors} = (\text{Length of path} - \text{Length of direct path})/2. \quad (7)$$

Statistics of sudden insight

In *Figure 4* one can distinguish two events: First the animal finds the water port and begins to collect rewards at a steady rate: this is when the green curve rises up. At a later time the long direct paths to the water port become much more frequent than to the comparable control nodes: this is when the red and blue curves diverge. For almost all animals these two events are well separated in time (*Figure 4-figure supplement 1*). In many cases the rate of long paths seems to change discontinuously: a sudden change in slope of the curve.

A sudden increase in the rate of certain behavioral events would suggest a sudden change in the animal’s strategy. Here we analyze the evidence for a sudden change in the time series of events. We focused on the occurrence of long paths to water, and compared two models: The “step model” supposes that the events are generated at a constant rate r_{before} up to some time t_s and then with a higher rate r_{after} ,

$$r_{\text{step}}(t) = \begin{cases} r_{\text{before}}, & t < t_s \\ r_{\text{after}}, & t > t_s \end{cases} \quad (8)$$

The “ramp model” supposes instead that the rate of the events increases in a graded fashion as

787 a quadratic function of time,

$$r_{\text{ramp}}(t) = a + bt + ct^2 \quad (9)$$

788 Note that each of the models has 3 free parameters. If the ramp model provides a better fit that
789 speaks against an interpretation in terms of “sudden insight”.

790 The data are a set of n event times t_i in the observation interval $[0, T]$. We model the event
791 train as an inhomogeneous Poisson point process with instantaneous rate $r(t)$. The likelihood
792 of the data given the rate function $r(t)$ is

$$L[r(t)] = e^{-\int_0^T r(t) dt} \prod_i r(t_i) \quad (10)$$

793 and the log likelihood is

$$\ln L = \sum_i \ln r(t_i) - \int_0^T r(t) dt \quad (11)$$

794 For each of the 10 rewarded mice, we maximized $\ln L$ over the parameters under both the
795 step model and the ramp model (*Figure 4-figure supplement 2*). For the step model, one can
796 optimize analytically with respect to the initial rate r_{before} and final rate r_{after} , and express the
797 log likelihood purely as a function of the step time t_s :

$$\ln L(t_s) = m(t_s) \ln m(t_s) + (n - m(t_s)) \ln (n - m(t_s)) - m(t_s) \ln t_s \\ - (n - m(t_s)) \ln (T - t_s) - n \quad (12)$$

798 where $m(t_s)$ is the number of events prior to the step time t_s . For the ramp model the optimization
799 was done by numerical search.

800 For 8 of 10 mice, the step model had a higher likelihood than the ramp model. For 5 mice,
801 the step model was more than 25 times as likely as the ramp model. In these 5 cases the change
802 in the frequency of long paths was large (5- to 1640-fold). The time of this step change in the
803 animal’s behavior ranged from 1280 to 2580 s in the maze, and could be identified with an
804 uncertainty of 80 to 310 s. This uncertainty is quoted as the standard deviation of the likelihood
805 expressed as a function of the step time (*Equation 12*).

806 Efficiency of exploration

807 The goal of this analysis is to measure how effectively the animal surveys all the end nodes of
808 the maze. The specific question is: In a string of n end nodes that the animal samples, how
809 many of these are distinct? On average how does the number of distinct nodes d increase with
810 n ? This was calculated as follows:

811 We restricted the animal’s node trajectory (s_i) to clips of exploration mode, excluding the
812 direct paths to the water port or the exit. All subsequent steps were applied to these clips, then
813 averaged over clips. Within each clip we marked the sequence of end nodes (e_i). We slid a
814 window of size n across this sequence and counted the number of distinct nodes d in each
815 window. Then we averaged d over all windows in all clips. Then we repeated that for a wide
816 range of n . The resulting $d(n)$ is plotted in the figures reporting new nodes vs nodes visited
817 (*Figure 7A,B and Figure 8C*).

818 For a summary analysis we fitted the curves of $d(n)$ with a 2-parameter function:

$$d(n) \approx 64 \left(1 - \frac{1}{1 + \frac{z+bz^3}{1+b}} \right) \quad (13)$$

819 where

$$z = n/a. \quad (14)$$

820 The parameter a is the number of visits n required to survey half of the end nodes, whereas b
821 reflects a relative acceleration in discovering the last few end nodes. This function was found
822 by trial and error and produces absurdly good fits to the data (*Figure 7-figure supplement 1*).
823 The values quoted in the text for efficiency of exploration are $E = 32/a$ (*Equation 1*).

824 The value of b was generally small (~ 0.1) with no difference between rewarded and unre-
825 wardered animals. It declined slightly over the night (*Figure 7-figure supplement 1B*), along
826 with the decline in a (*Figure 7C*).

827 Biased random walk

828 For the analysis of *Figure 8* we considered only the parts of the trajectory during ‘exploration’
829 mode. Then we parsed every step between two nodes in terms of the type of action it represents.
830 Note that every link between nodes in the maze is either a ‘left branch’ or a ‘right branch’,
831 depending on its relationship to the parent T-junction. Therefore there are 4 kinds of action:

- 832 • $a = 0$: ‘in left’, take a left branch into the maze
- 833 • $a = 1$: ‘in right’, take a right branch into the maze
- 834 • $a = 2$: ‘out left’, take a left branch out of the maze
- 835 • $a = 3$: ‘out right’, take a right branch out of the maze

836 At any given node some actions are not available, for example from an end node one can
837 only take one of the ‘out’ actions.

838 To compute the turning biases we considered every T-junction along the trajectory and
839 correlated the action a_0 that led into that node with the subsequent action a_1 . By tallying the
840 action pairs (a_0, a_1) we computed the conditional probabilities $p(a_1|a_0)$. Then the 4 biases are
841 defined as

$$P_{SF} = \frac{p(0|0) + p(0|1) + p(1|0) + p(1|1)}{p(0|0) + p(0|1) + p(1|0) + p(1|1) + p(2|0) + p(3|1)} \quad (15)$$

$$P_{SA} = \frac{p(0|1) + p(1|0)}{p(0|0) + p(0|1) + p(1|0) + p(1|1)} \quad (16)$$

$$P_{BF} = \frac{p(0|3) + p(1|2) + p(2|2) + p(2|3) + p(3|2) + p(3|3)}{p(0|3) + p(1|2) + p(2|2) + p(2|3) + p(3|2) + p(3|3) + p(0|2) + p(1|3)} \quad (17)$$

$$P_{BS} = \frac{p(2|2) + p(2|3) + p(3|2) + p(3|3)}{p(0|3) + p(1|2) + p(2|2) + p(2|3) + p(3|2) + p(3|3)} \quad (18)$$

842 Models of decisions during exploration

843 The general approach is to develop a model that assigns probabilities to the animal’s next
844 action, namely which node it will move to next, based on its recent history of actions. All the
845 analysis was restricted to the animal’s ‘exploration’ mode and to the 63 nodes in the maze that
846 are T-junctions. During the ‘drink’ and ‘leave’ modes the animal’s next action is predictable.
847 Similarly when it finds itself at one of the 64 end nodes it only has one action available.

For every mouse trajectory we split the data into 5 segments, trained the model on 80% of the data, and tested it on 20%, averaging the resulting cross-entropy over the 5 possible splits. Each segment was in turn composed of parts of the trajectory sampled evenly throughout the 7-h experiment, so as to average over the small changes in the course of the night. The model was evaluated by the cross-entropy between the predictions and the animal's true actions. If one had an optimal model of behavior, the result would reveal the animal's true source entropy.

Fixed depth Markov chain

To fit a model with fixed history depth k to a measured node sequence (s_t) , we evaluated all the substrings in that sequence of length $(k + 1)$. At any given time t , the k -string $\mathbf{h}_t = (s_{t-k+1}, \dots, s_t)$ identifies the history of the animal's k most recent locations. The current state s_t is one of 63 T-junctions. Each state is preceded by one of 3 possible states. So the number of history strings is $63 \cdot 3^{k-1}$. The 2-string (s_t, s_{t+1}) identifies the next action a_{t+1} , which can be 'in left', 'in right', or 'out', corresponding to the 3 branches of the T junction. Tallying the history strings with the resulting actions leads to a contingency table of size $63 \cdot 3^{k-1} \times 3$, containing

$$n(\mathbf{h}, a) = \text{number of times history } \mathbf{h} \text{ leads to action } a \quad (19)$$

Based on these sample counts we estimated the probability of each action a conditional on the history \mathbf{h} as

$$p(a | \mathbf{h}) = \frac{n(\mathbf{h}, a) + 1}{\sum_{a'} n(\mathbf{h}, a') + 3} \quad (20)$$

This amounts to additive smoothing with a pseudocount of 1, also known as "Laplace smoothing". These conditional probabilities were then used in the testing phase to predict the action at time t based on the preceding history \mathbf{h}_t . The match to the actually observed actions a_t was measured by the cross-entropy

$$H = - \sum_t \log_2 p(a_t | \mathbf{h}_t) \quad (21)$$

Variable depth Markov chain

As one pushes to longer histories, i.e. larger k , the analysis quickly becomes data-limited, because the number of possible histories grows exponentially with k . Soon one finds that the counts for each history-action combination drop to where one can no longer estimate probabilities correctly. In an attempt to offset this problem we pruned the history tree such that each surviving branch had more than some minimal number of counts in the training data.

As expected, this model is less prone to over-fitting and degrades more gently as one extends to longer histories (*Figure 10-figure supplement 1A*). The lowest cross-entropy was obtained with an average history length of ~ 4.0 but including some paths of up to length 6. Of all the algorithms we tested, this produced the lowest cross-entropies, although the gains relative to the fixed-depth model were modest (*Figure 10-figure supplement 1C*).

Pooling across symmetric nodes in the maze

Another attempt to increase the counts for each history involved pooling counts over multiple T-junctions in the maze that are closely related by symmetry. For example, all the T-junctions at the same level of the binary tree look locally similar, in that they all have corridors of identical length leading from the junction. If one supposes that the animal acts the same way at each of those junctions, one would be justified in pooling across these nodes, leading to a better

estimate of the action probabilities, and perhaps less over-fitting. This particular procedure was unsuccessful, in that it produced higher cross-entropy than without pooling.

However, one may want to distinguish two types of junctions within a given level: L-nodes are reached by a left branch from their parent junction one level lower in the tree, R-nodes by a right branch. For example, in *Figure 3-figure supplement 1*, node 1 is L-type and node 2 is R-type. When we pooled histories over all the L-nodes at a given level and separately over all the R-nodes the cross-entropy indeed dropped, by about 5% on average. This pooling greatly reduced the amount of over-fitting (*Figure 10-figure supplement 1B*), which allowed the use of longer histories, which in turn improved the predictions on test data. The benefit of distinguishing L- and R-nodes probably relates to the animal's tendency to alternate left and right turns.

All the Markov model results we report are obtained using pooling over L-nodes and R-nodes at each maze level.

Data availability

All data and code needed to reproduce the figures and quoted results are available in this public repository: <https://github.com/markusmeister/Rosenberg-2021-Repository>.

Acknowledgments

Funding: This work was supported by the Simons Collaboration on the Global Brain (grant 543015 to MM and 543025 to PP), by NSF award 1564330 to PP, and by a gift from Google to PP.

Author contributions: Conception of the study MR, TZ, PP, MM; Data collection MR, TZ; Analysis and interpretation MR, TZ, PP, MM; Drafting the manuscript MM; Revision and approval MR, TZ, PP, MM.

Competing interests: The authors declare no competing interests.

Data and code availability: Data and code will be available in a public repository following acceptance of the manuscript.

References

- Behrens TEJ, Muller TH, Whittington JCR, Mark S, Baram AB, Stachenfeld KL, Kurth-Nelson Z. What Is a Cognitive Map? Organizing Knowledge for Flexible Behavior. *Neuron*. 2018 Oct; 100(2):490–509. doi: 10.1016/j.neuron.2018.10.002.
- Berlyne DE. Conflict, Arousal, and Curiosity. New York, NY, US: McGraw-Hill Book Company; 1960. doi: 10.1037/11164-000.
- Bitterman ME, Menzel R, Fietz A, Schäfer S. Classical Conditioning of Proboscis Extension in Honeybees (*Apis Mellifera*). *Journal of Comparative Psychology*. 1983; 97(2):107–119. doi: 10.1037/0735-7036.97.2.107.
- Bourtchuladze R, Frenguelli B, Blendy J, Cioffi D, Schutz G, Silva AJ. Deficient Long-Term Memory in Mice with a Targeted Mutation of the cAMP-Responsive Element-Binding Protein. *Cell*. 1994 Oct; 79(1):59–68. doi: 10.1016/0092-8674(94)90400-6.
- Brennan PA, Keverne EB. Neural Mechanisms of Mammalian Olfactory Learning. *Progress in Neurobiology*. 1997 Mar; 51(4):457–481. doi: 10.1016/s0301-0082(96)00069-x.
- Bruce HM. An Exteroceptive Block to Pregnancy in the Mouse. *Nature*. 1959 Jul; 184:105. doi: 10.1038/184105a0.
- Buel J. The Linear Maze. I. "Choice-Point Expectancy," "Correctness," and the Goal Gradient. *Journal of Comparative Psychology*. 1934; 17(2):185–199. doi: 10.1037/h0072346.
- Burgess CP, Lak A, Steinmetz NA, Zátka-Haas P, Bai Reddy C, Jacobs EAK, Linden JF, Paton JJ, Ranson A, Schröder S, Soares S, Wells MJ, Wool LE, Harris KD, Carandini M. High-Yield Methods for Accurate Two-Alternative Visual Psychophysics in Head-Fixed Mice. *Cell Reports*. 2017 Sep; 20(10):2513–2524. doi: 10.1016/j.celrep.2017.08.047.
- Carandini M, Churchland AK. Probing Perceptual Decisions in Rodents. *Nature Neuroscience*. 2013 Jul; 16:824–31. doi: 10.1038/nn.3410.
- Cleland TA, Narla VA, Boudadi K. Multiple Learning Parameters Differentially Regulate Olfactory Generalization. *Behavioral Neuroscience*. 2009 Feb; 123(1):26–35. doi: 10.1037/a0013991.
- Estes W. The Problem of Inference from Curves Based on Group Data. *Psychological Bulletin*. 1956; 53(2):134–140. doi: 10.1037/h0045156.
- Fanselow M, Bolles R. Naloxone and Shock-Elicited Freezing in the Rat. *Journal of comparative and physiological psychology*. 1979 Sep; 93:736–44. doi: 10.1037/h0077609.
- Fonio E, Benjamini Y, Golani I. Freedom of Movement and the Stability of Its Unfolding in Free Exploration of Mice. *Proceedings of the National Academy of Sciences of the United States of America*. 2009 Dec; 106(50):21335–21340. doi: 10.1073/pnas.0812513106.
- Gallistel CR, Fairhurst S, Balsam P. The Learning Curve: Implications of a Quantitative Analysis. *Proceedings of the National Academy of Sciences of the United States of America*. 2004 Sep; 101(36):13124–13131. doi: 10.1073/pnas.0404965101.
- Guo ZV, Li N, Huber D, Ophir E, Gutnisky D, Ting JT, Feng G, Svoboda K. Flow of Cortical Activity Underlying a Tactile Decision in Mice. *Neuron*. 2014 Jan; 81(1):179–194. doi: 10.1016/j.neuron.2013.10.020.
- Hughes RN. Intrinsic Exploration in Animals: Motives and Measurement. *Behavioural Processes*. 1997 Dec; 41(3):213–226. doi: 10.1016/S0376-6357(97)00055-7.
- Kim SM, Frank LM. Hippocampal Lesions Impair Rapid Learning of a Continuous Spatial Alternation Task. *PLOS ONE*. 2009 May; 4(5):e5494. doi: 10.1371/journal.pone.0005494.

- 952 **Krechevsky I.** "Hypotheses" in Rats. *Psychological Review*. 1932; 39(6):516–532. doi:
953 10.1037/h0073500.
- 954 **LeDoux JE.** Emotion Circuits in the Brain. *Annual Review of Neuroscience*. 2000; 23:155–184. doi:
955 10.1146/annurev.neuro.23.1.155.
- 956 **Munn NL.** The Learning Process. In: *Handbook of Psychological Research on the Rat; an Introduction*
957 *to Animal Psychology* Oxford, England: Houghton Mifflin; 1950.p. 226–288.
- 958 **Munn NL.** The Role of Sensory Processes in Maze Behavior. In: *Handbook of Psychological Research*
959 *on the Rat; an Introduction to Animal Psychology* Oxford, England: Houghton Mifflin; 1950.p.
960 181–225.
- 961 **Nagy M,** Horicsányi A, Kubinyi E, Couzin ID, Vásárhelyi G, Flack A, Vicsek T. Synergistic Benefits
962 of Group Search in Rats. *Current Biology*. 2020 Sep; doi: 10.1016/j.cub.2020.08.079.
- 963 **Nath T,** Mathis A, Chen AC, Patel A, Bethge M, Mathis MW. Using DeepLabCut for 3D Markerless
964 Pose Estimation across Species and Behaviors. *Nature Protocols*. 2019 Jul; 14(7):2152–2176. doi:
965 10.1038/s41596-019-0176-0.
- 966 **Newsome WT,** Pare EB. A Selective Impairment of Motion Perception Following Lesions of the
967 Middle Temporal Visual Area (MT). *Journal of Neuroscience*. 1988 Jun; 8(6):2201–2211. doi:
968 10.1523/JNEUROSCI.08-06-02201.1988.
- 969 **Olton D.** Mazes, Maps, and Memory. *American Psychologist*. 1979; 34(7):583–596. doi: 10.1037/0003-
970 066X.34.7.583.
- 971 **Pseudo-Apollodorus.** Epitome. In: *Library and Epitome*; 1st Century AD?.p. Ch 1 Sec 9.
- 972 **Rosser AE,** Keverne EB. The Importance of Central Noradrenergic Neurones in the Formation of an
973 Olfactory Memory in the Prevention of Pregnancy Block. *Neuroscience*. 1985 Aug; 15(4):1141–1147.
974 doi: 10.1016/0306-4522(85)90258-1.
- 975 **Seward J,** Bzip2; 2019.
- 976 **Small WS.** Experimental Study of the Mental Processes of the Rat. II. The American Journal of
977 Psychology. 1901; 12(2):206–239. doi: 10.2307/1412534.
- 978 **Tolman EC.** The Determiners of Behavior at a Choice Point. *Psychological Review*. 1938; 45:1–41.
979 doi: 10.1037/h0062733.
- 980 **Tolman EC.** Cognitive Maps in Rats and Men. *Psychological Review*. 1948; 55(4):189–208. doi:
981 10.1037/h0061626.
- 982 **Tolman E,** Honzik C. Degrees of Hunger, Reward and Non-Reward, and Maze Learning in Rats.
983 University of California Publications in Psychology. 1930; 4:241–256.
- 984 **Uchida N,** Mainen ZF. Speed and Accuracy of Olfactory Discrimination in the Rat. *Nature Neuroscience*.
985 2003 Nov; 6(11):1224–1229. doi: 10.1038/nn1142.
- 986 **Uster HJ,** Bättig K, Nägeli HH. Effects of Maze Geometry and Experience on Exploratory Behavior in
987 the Rat. *Animal Learning & Behavior*. 1976 Mar; 4(1):84–88. doi: 10.3758/BF03211992.
- 988 **Weber JN,** Peterson BK, Hoekstra HE. Discrete Genetic Modules Are Responsible for Complex Burrow
989 Evolution in *Peromyscus* Mice. *Nature*. 2013 Jan; 493(7432):402–405. doi: 10.1038/nature11816.
- 990 **Wehner R,** Michel B, Antonsen P. Visual Navigation in Insects: Coupling of Egocentric and Geocentric
991 Information. *Journal of Experimental Biology*. 1996 Jan; 199(1):129–140.
- 992 **Woodrow H.** The Problem of General Quantitative Laws in Psychology. *Psychological Bulletin*. 1942;
993 39(1):1–27. doi: 10.1037/h0058275.

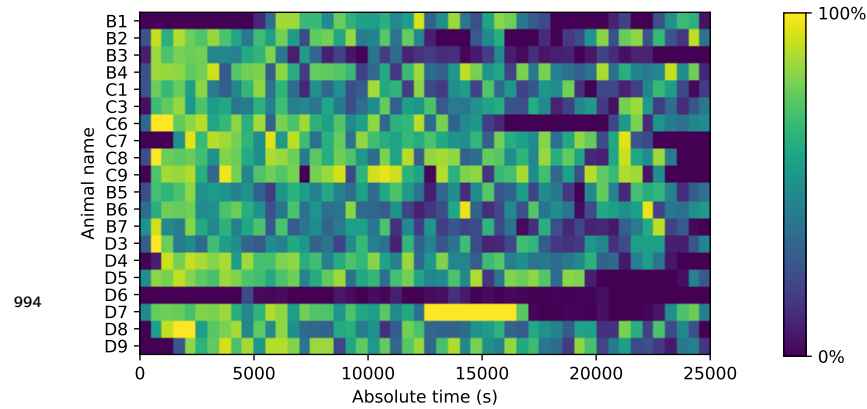


Figure 1-figure supplement 1. Fraction of time spent in the maze. Mice could move freely between the home cage and the maze. For each animal (vertical), the fraction of time in the maze (color scale) is plotted as a function of time since start of the experiment. Time bins are 500 s. Note that mouse D6 hardly entered the maze; it never progressed beyond the first junction. This animal was excluded from all subsequent analysis steps.

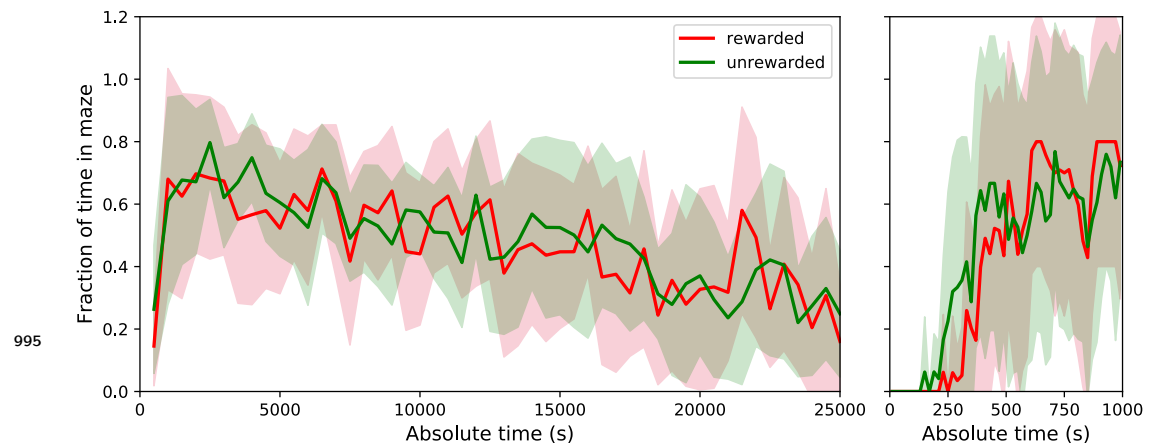


Figure 1-figure supplement 2. Average fraction of time spent in the maze by group. This shows the average fraction of time in the maze as Mean \pm SD over the population of 10 rewarded and 9 unrewarded animals. Right: expanded axis for early times. The tunnel to the maze opens at time 0. Rewarded and unrewarded animals used the maze in remarkably similar ways. Exploration of the maze began around 250 s after tunnel opening. Within the next 250 s the maze occupancy rose quickly to ~70%, then declined gradually over 7 h to ~30%.

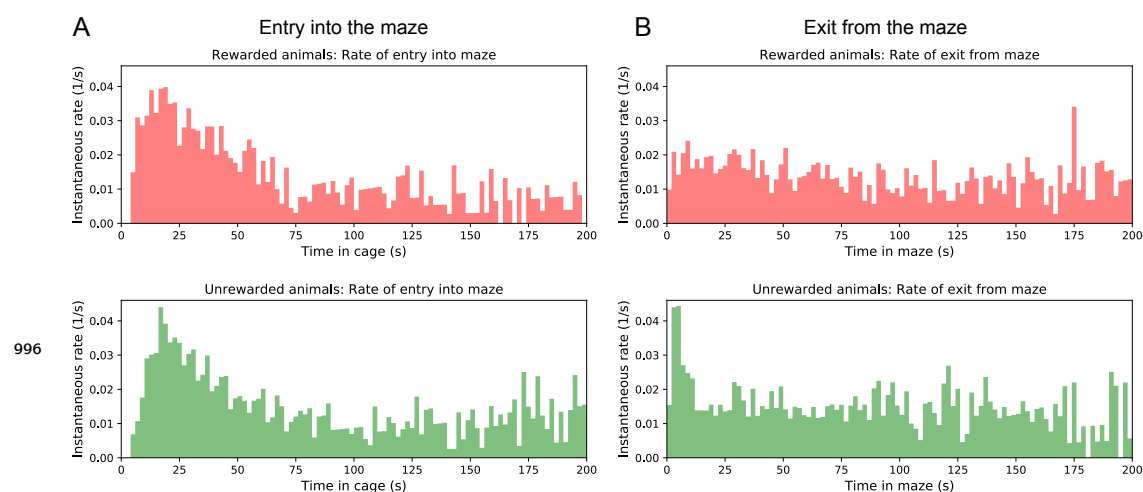


Figure 1-figure supplement 3. Rates of transition between cage and maze. (A) The instantaneous probability per unit time $r_m(t)$ of entering the maze after having spent time t in the cage. Note this rate is highest immediately upon entering the cage, then declines by a large factor. (B) The instantaneous probability per unit time $r_c(t)$ of exiting the maze after having spent time t in the maze.

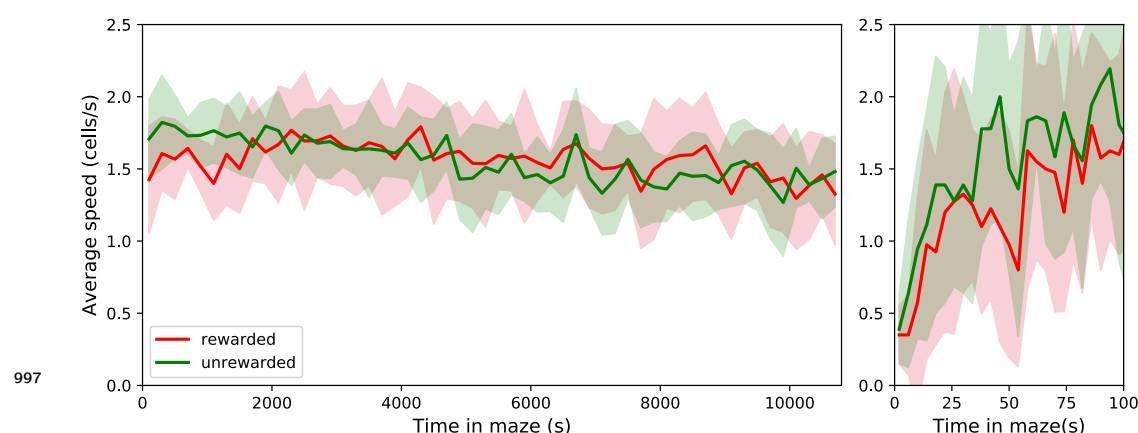


Figure 2-figure supplement 1. The speed of locomotion in the maze is approximately constant. Left: Speed plotted as Mean \pm SD over the population of rewarded and unrewarded animals. Right: expanded axis for early times. To assess the speed of locomotion we divided the maze into square cells as wide as the corridors and tracked how the nose of the animal moved through those cells. Then the speed was measured in number of cells traversed per unit time. Note that the speed is very similar across animals, ~ 1.56 cells/s = 5.94 cm/s on average. It rises quickly over the first 50 s in the maze, then varies only little over the 7 h of the experiment.



Figure 3-figure supplement 1. Definition of node trajectories. A numbering scheme for all 127 nodes of the maze. Green: a direct path from the entrance to the water port (“water run”) with the node sequence $(s_i) = (0, 2, 6, 13, 28, 57, 116)$, involving 6 decisions. Magenta: a direct path from end node 83 to the exit (“home run”). Orange: a path from end node 67 to the exit that includes a reversal. Here the home run starts only from node 8, namely $(8, 3, 1, 0)$.

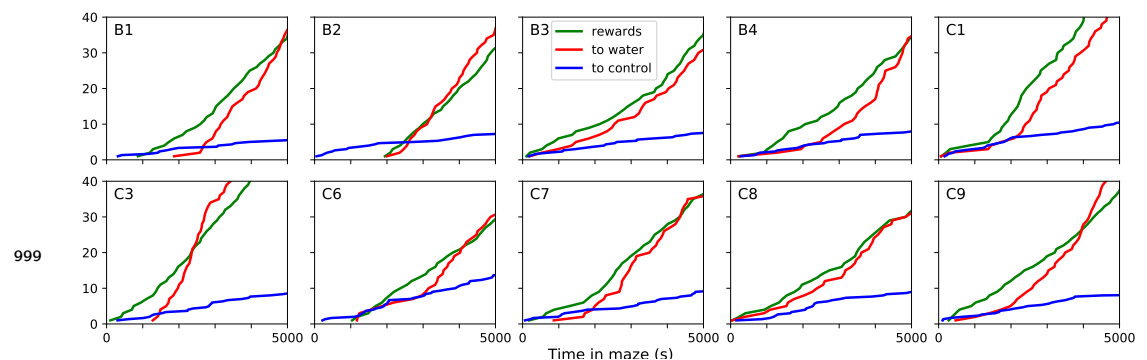


Figure 4-figure supplement 1. Sudden changes in behavior for all rewarded animals. For each of the 10 water-deprived animals this shows the cumulative rate of rewards, of long direct paths (>6 steps) to the water port, and of similar paths to 3 control nodes. Display as in Figure 4; panels B and C of that figure are included again here.

Animal	Likelihood ratio step/ramp	Time of step (s)	Ratio of rates after/before
B1	25.1	2580 ± 110	36.4
B2	36.2	2350 ± 220	30.3
B3	1.61	3090 ± 970	2.77
B4	0.67	2490 ± 590	7.36
C1	25.8	2070 ± 310	5.49
C3	32900	1280 ± 80	1640
C6	2.31	2960 ± 890	4.75
C7	41.3	1680 ± 280	16.9
C8	3.52	3070 ± 1000	2.50
C9	0.44	1980 ± 560	6.69

Figure 4—figure supplement 2. Statistics of sudden changes in behavior. Summary of ‘step’ and ‘ramp’ models fitted to the occurrence of long direct paths to the water port for all 10 rewarded animals. Boldface animals have a likelihood ratio > 25.

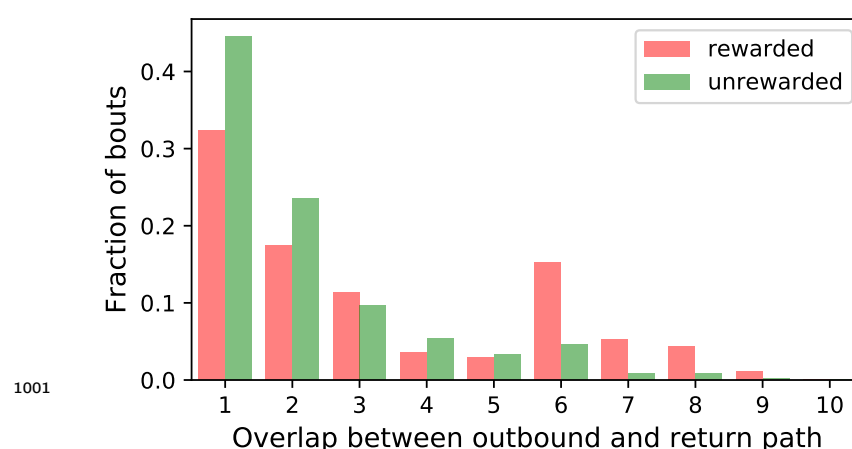


Figure 5—figure supplement 1. Entry paths do not retrace exit paths. For every bout we compared the start of the node sequence leading into the maze with the final portion leading back out to the exit. The number of nodes of the entry sequence that match the time-reverse of the exit sequence is called the “overlap”. This figure histograms the overlap for all bouts of all animals. Note the minimum overlap is 1, because all paths into and out of the maze have to pass through the central junction (node 0 in *Figure 3—figure supplement 1*). This is also the most frequent overlap. The peak at overlap 6 for rewarded animals results from the frequent direct paths to the water port and back, a sequence of 6 nodes in each direction.

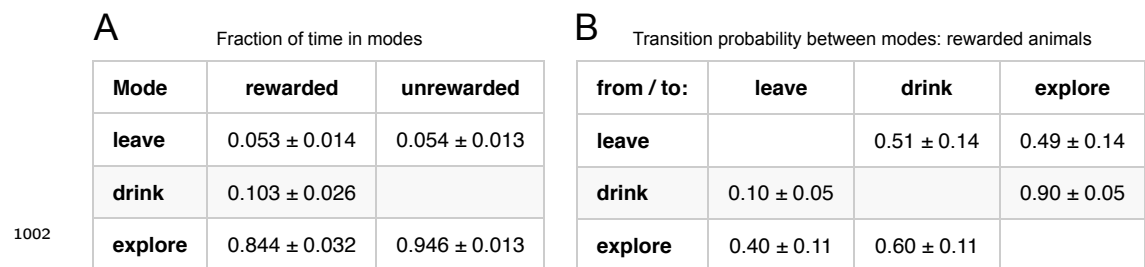


Figure 6—figure supplement 1. Three modes of behavior. (A) The fraction of time mice spent in each of the three modes while in the maze. Mean \pm SD for 10 rewarded and 9 unrewarded animals. (B) Probability of transitioning from the mode on the left to the mode at the top. Transitions from ‘leave’ represent what the animal does at the start of the next bout into the maze.

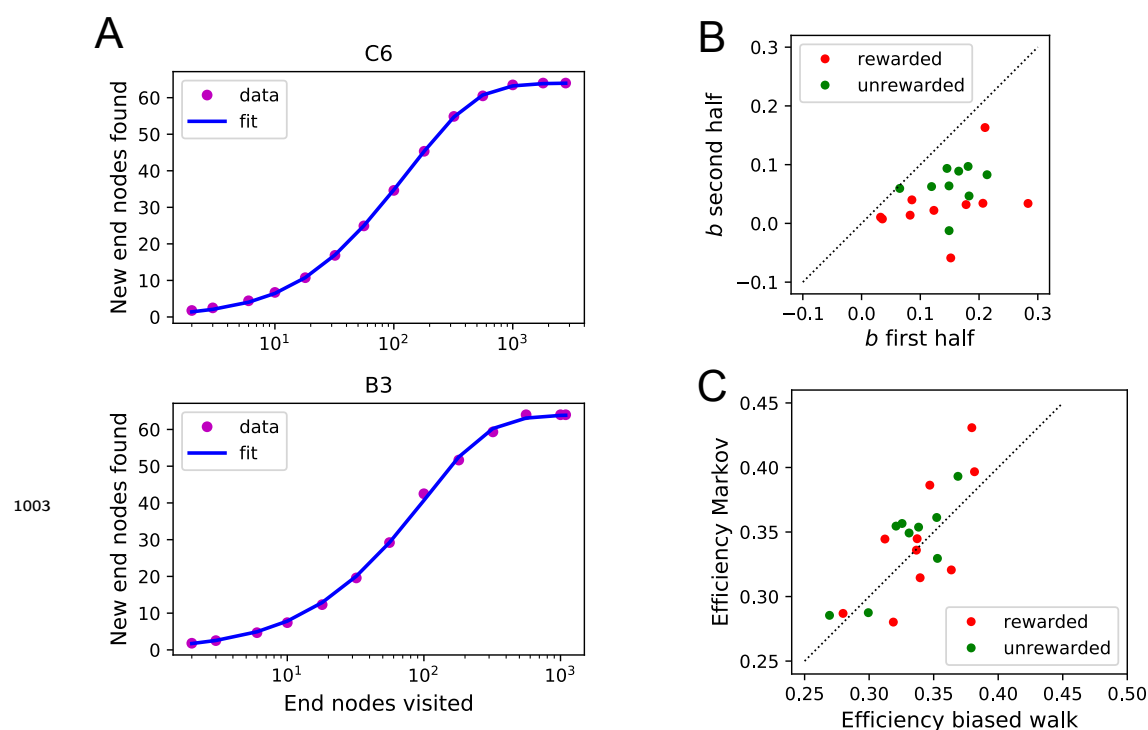


Figure 7—figure supplement 1. Functional fits to measure exploration efficiency (A) Fitting Equation 13 to the data from the mouse’s exploration. Animals with best fit (top) and worst fit (bottom). The relative uncertainty in the two fit parameters a and b was only 0.0038 ± 0.0020 (mean \pm SD across animals). (B) The fit parameter b for all animals, comparing the first to the second half of the night. (C) The efficiency E (Equation 1) predicted from two models of the mouse’s trajectory: The 4-bias random walk (Figure 10D) and the optimal Markov chain (Figure 10C).

Bias	rewarded	unrewarded
P_{SF}	0.77 ± 0.03	0.78 ± 0.02
P_{SA}	0.72 ± 0.02	0.71 ± 0.02
P_{BF}	0.82 ± 0.03	0.81 ± 0.03
P_{BS}	0.64 ± 0.02	0.63 ± 0.02

Figure 8—figure supplement 1. Statistics of the four turning biases. Mean and standard deviation of the 4 biases of Figure 8A-B across animals in the rewarded and unrewarded groups.

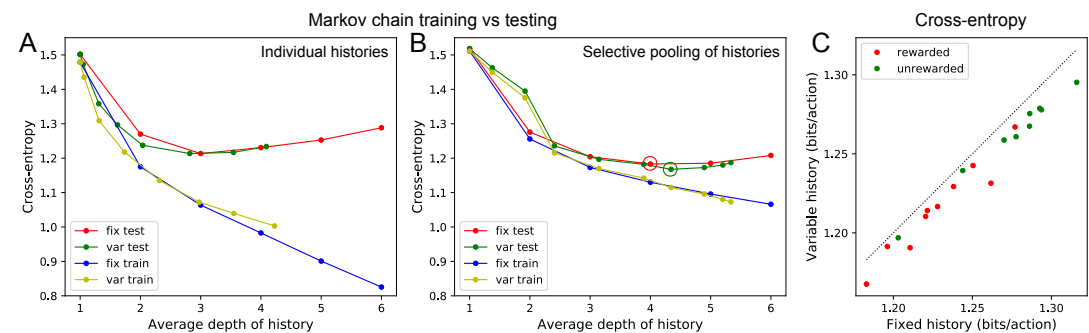


Figure 10—figure supplement 1. Fitting Markov models of behavior. (A) Results of fitting the node sequence of a single animal (C3) with Markov models having a fixed depth ('fix') or variable depth ('var'). The cross-entropy of the model's prediction is plotted as a function of the average depth of history. In both cases we compare the results obtained on the training data ('train') vs those on separate testing data ('test'). Note that at larger depth the 'test' and 'train' estimates diverge, a sign of over-fitting the limited data available. (B) As in (A) but to combat the data limitation we pooled the counts obtained at all nodes that were equivalent under the symmetry of the maze (see Methods). Note considerably less divergence between 'train' and 'test' results, and a slightly lower cross-entropy during 'test' than in (A). (C) The minimal cross-entropy (circles in (B)) produced by variable vs fixed history models for each of the 19 animals. Note the variable history model always produces a better fit to the behavior.